大阪大學

共鳴軟X線回折のマルチフェロイック関連物質への適用

大阪大学基礎工学研究科　木村 剛

Acknowledgements

薄井智靖, 中島宏, 上田大貴, 平岡裕治, 若林裕助 （阪大基礎工）

田中良和, 大浦正樹, 田口宗孝, A. Chainani, 辛埴 （理研播磨研）

仙波泰徳, 大橋治彦 （高輝度光科学研究センター）

小山司, 戸川欣彦, 森茂生 （阪府大工）

片山尚幸, 澤博大 （名大工）

(Magnetoelectric) Multiferroics

Materials which exhibit two or all three ferroic orders

ferro-elastic, <u>ferro-magnetic</u>, <u>ferro-electric</u>

空間反転対称性の破れ

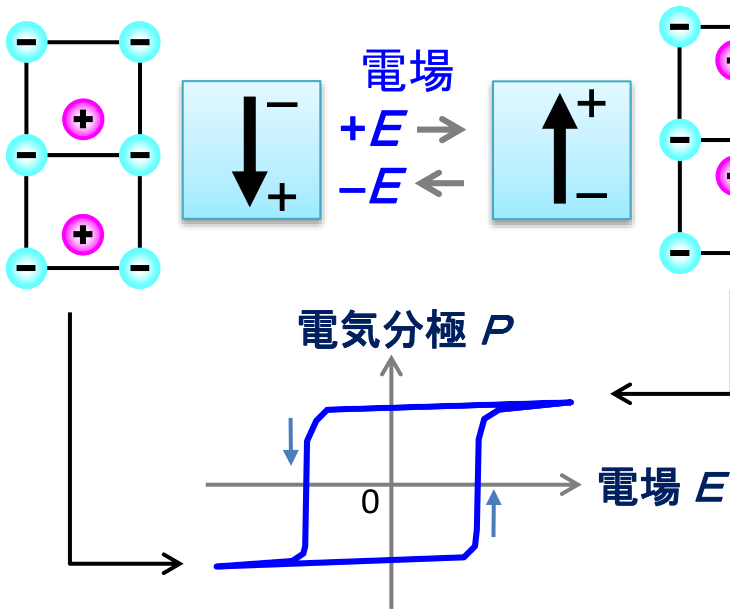

強誘電性 (Ferro-electric)

時間反転対称性の破れ

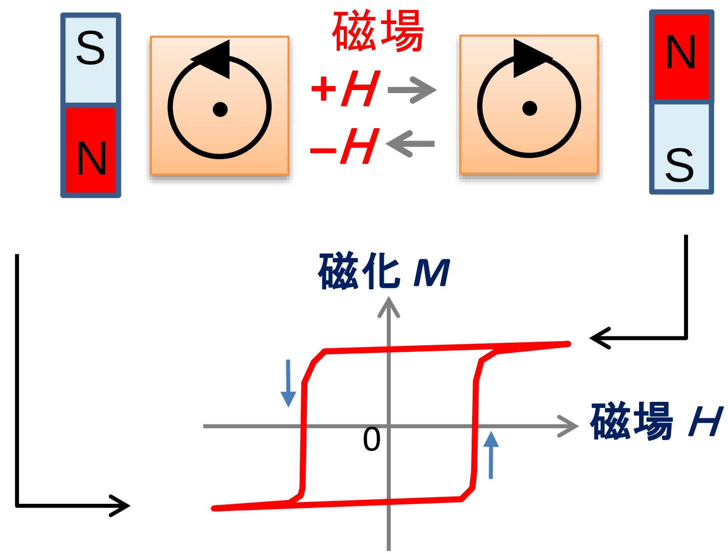

強磁性 (Ferro-magnetic)

空間反転対称性と時間反転対称性の両方が同時に破れた系

(Magnetoelectric) Multiferroics

- 空間反転対称性と時間反転対称性の両方が同時に破れた系

- スピン配列によって空間(+時間)反転対称性が破れた系

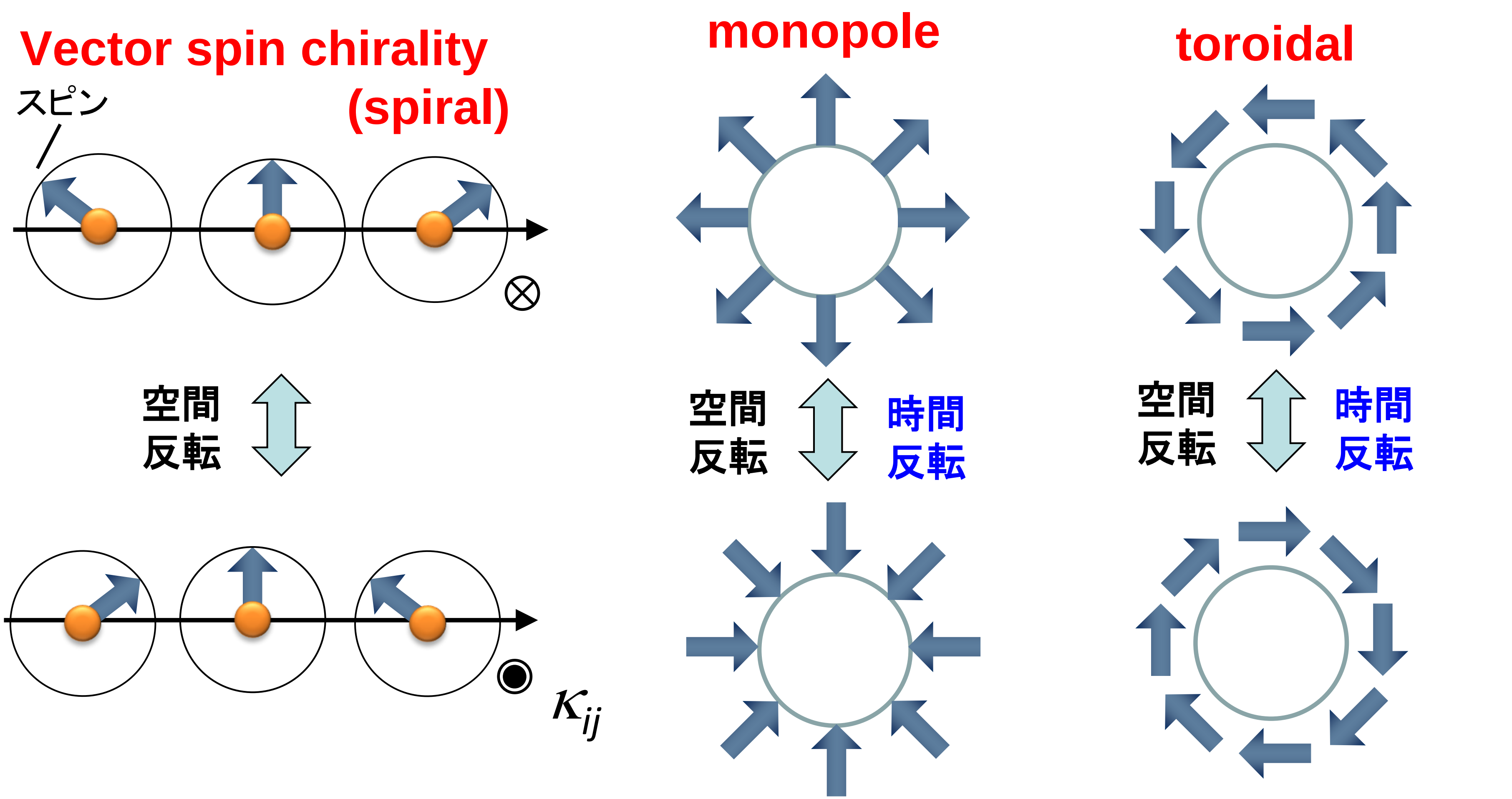

電気磁気効果の発現、ドメイン構造の形成

Observation of multiferroic domains

Second harmonic generation (第2高調波発生)

spin chirality $TbMnO_3$

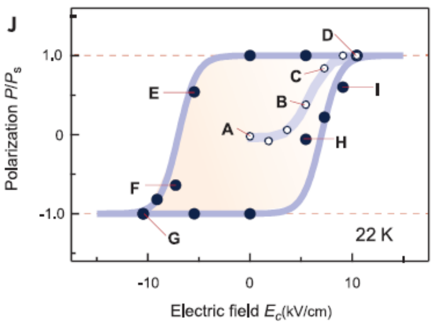

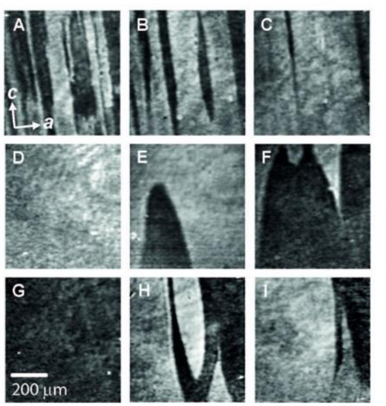

Matsubara et al. Science 348, 1112 (2015).

monopole Cr_2O_3

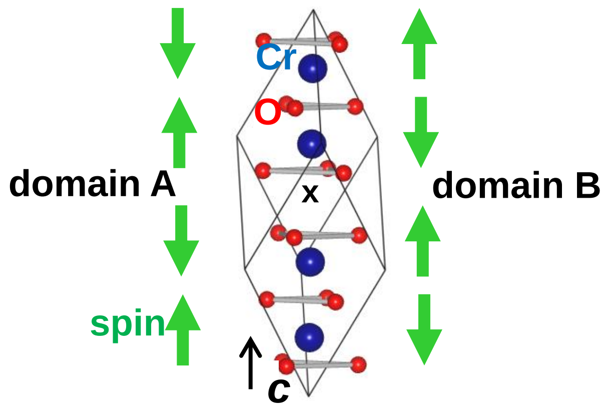

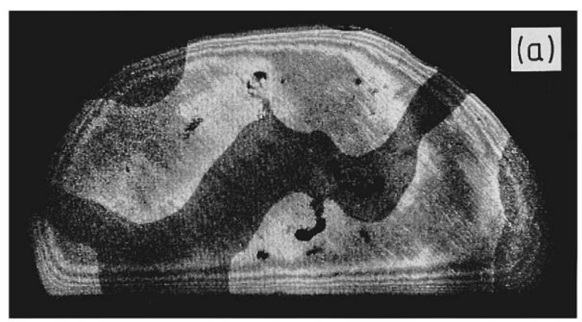

Fiebig et al., APL 66, 2906 (1995).

toroidal $LiCoPO_4$

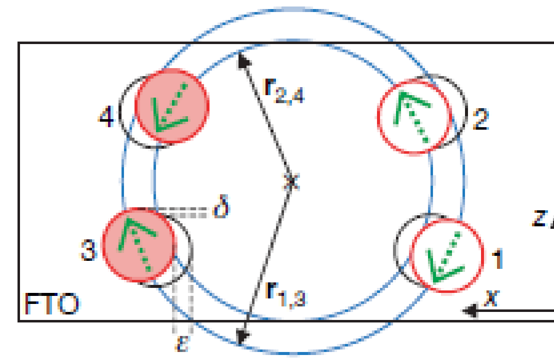

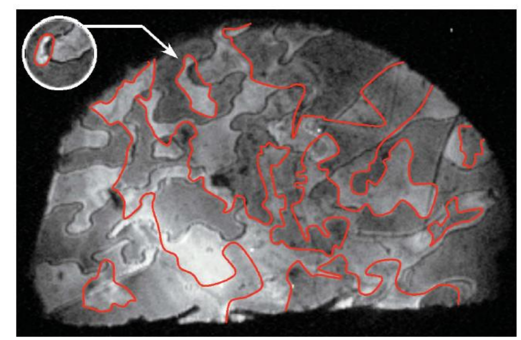

Van Aken et al. Nature 449, 702 (2007)

Chirality formed by multipole moments

Spin (magnetic dipole)

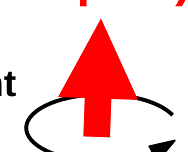

Electric quadrupole

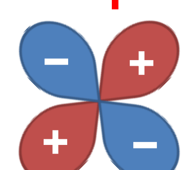

Outline of this presentation

Observation of multipole helix-chiral domains
by resonant soft x-ray scattering

1. Resonant x-ray diffraction using circularly polarized x-rays
   a technique to verify symmetry breaking due to chirality

2. Chiral domains due to magnetic dipoles in multiferroic
   Y-type hexaferrites $(Ba,Sr)_2Z(Co,Zn)_2(Fe,Al)_{12}O_{22}$

3. Chiral domains due to electric quadrupoles
   in enantiomophic ferroborate $DyFe_3(BO_3)_4$

4. Summary

Resonant x-ray diffraction using soft x-rays

ATS scattering

Anisotropy of tensor of susceptibility

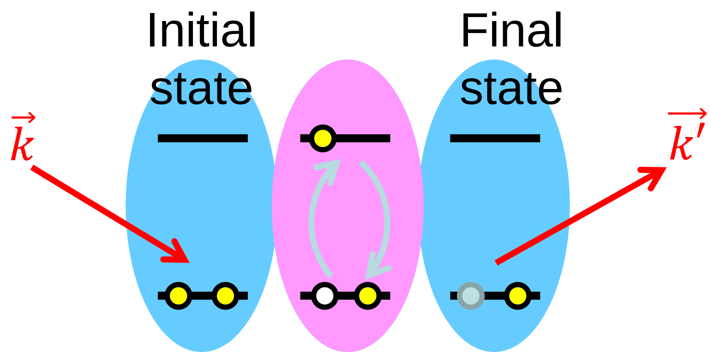

Intermediate state
(resonance)

$f = f_0 + f' + if''$

Anisotropy of unoccupied states at resonant atom

Observation of forbidden reflection

Scattering intensity: $I \propto |F|^2$

$$F = \sum_j f_j \exp i(\boldsymbol{\kappa} \cdot \boldsymbol{r}_j)$$

Structure factor

Atomic scattering factor

Phase factor

$\langle T_Q^K \rangle$: **multipole** (spherical tensor)

○ Soft x-ray region (100~2000 eV)

(6.2Å~124Å)

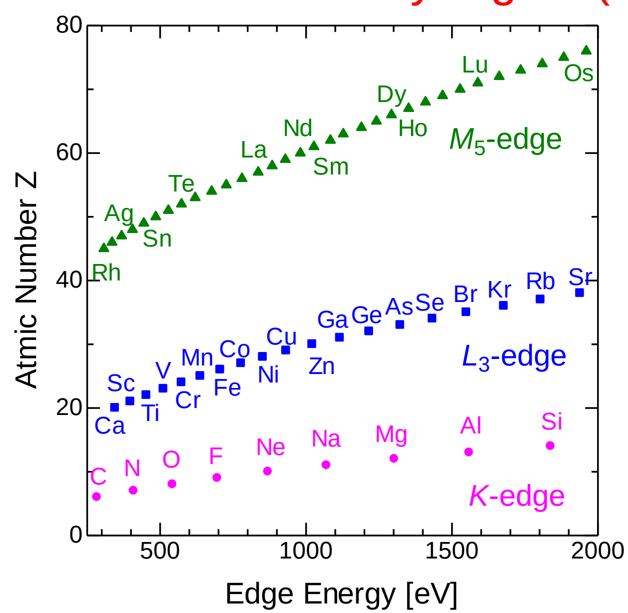

4f M_5 edges
$3d \rightarrow 4f$

3d L_3 edges
$2p \rightarrow 3d$

Light element K edges
$1s \rightarrow 4p$

e.g., Observation of multipole orders (e.g. electric monopole, magnetic dipole, electric quadrupole,…)

Resonant x-ray diffraction using circularly polarized soft x-ray

Using strong polarization dependence of ATS scattering

RXD + Circularly polarized x-rays

Correlation between X-ray's helicity & Chirality in crystal

Crystallographic chirality can be verified.

When an observer looks the beam source, E of + helicity beam is counterclockwise in time and has a left-handed screw-in space.

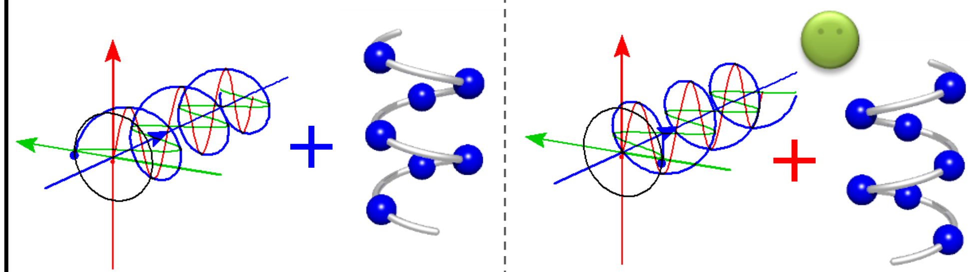

Helicity(-) + Left-screw

Helicity(+) + Right-screw

Strong scattering

3-fold helix (3_1 or 3_2) ⇨ **SiO_2**

Y. Tanaka et. al , PRL 100, 145502 (2008)

6-fold helix (6_1 or 6_5) ⇨ **$CsCuCl_3$**

Y. Kousaka et al., JPSJ 78 (2009) 123601 **(Hard X-ray)**

H. Ohsumi et al., Angew. Chem.125, 1 (2013)

Quartz SiO_2

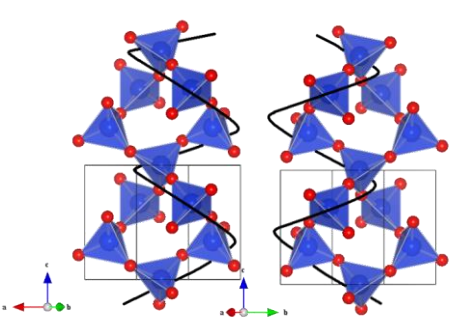

L-SiO_2 $P3_221$

R-SiO_2 $P3_121$

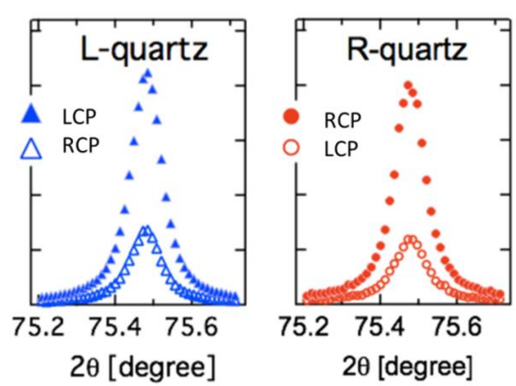

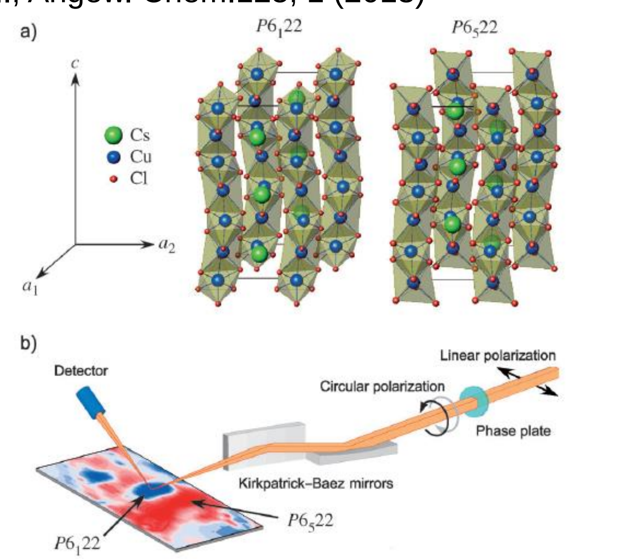

Imaging spiral magnetic domains in Ho by circularly polarized Bragg diffraction

J.C. Lang et al., J. Appl. Phys. 95, 6537 (2004).

Ho metal

[spiral magnetic order with (0,0, $L \pm \tau$) below T_N=133K]

X-ray energy E~ 8.071 eV (~ Ho L_3-edge 2p → 5d)

Size of circularly polarized x-ray beam

25 μm × 25μm

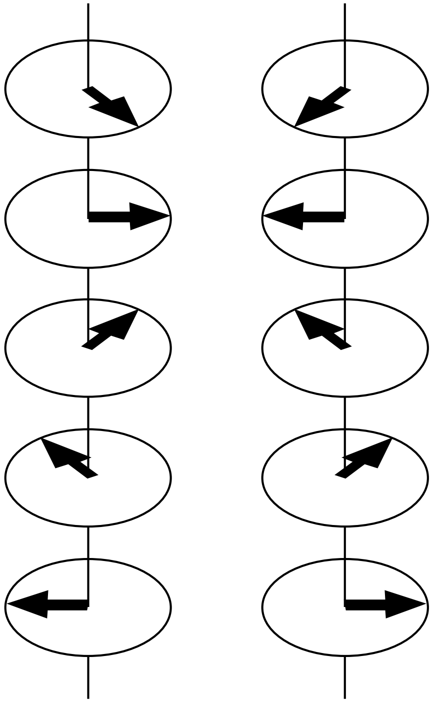

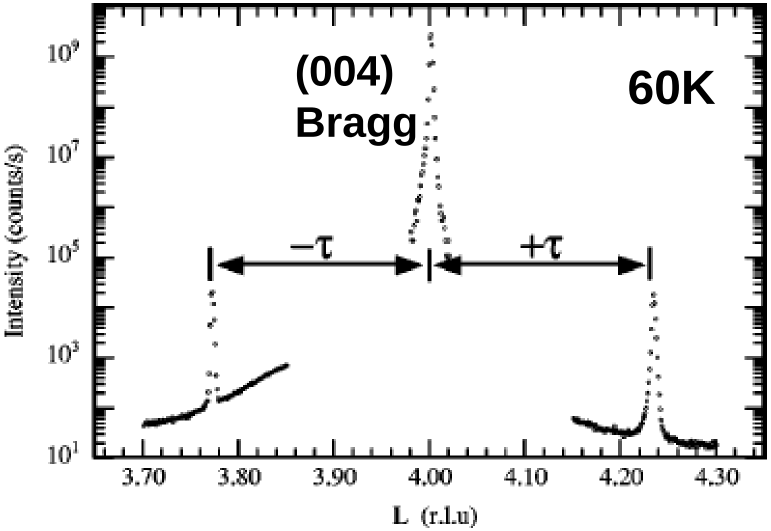

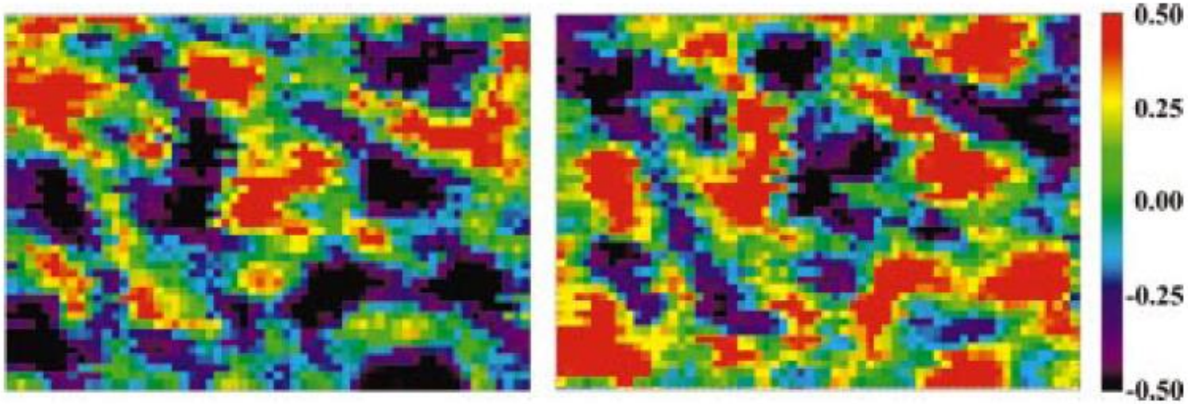

(0.6X0.45mm^2)

Outline of this presentation

Observation of multipole helix-chiral domains by resonant soft x-ray scattering

1. Resonant x-ray diffraction using circularly polarized x-rays
   a technique to verify symmetry breaking due to chirality

2. Chiral domains due to magnetic dipoles in multiferroic
   Y-type hexaferrites $(Ba,Sr)_2Z(Co,Zn)_2(Fe,Al)_{12}O_{22}$

3. Chiral domains due to electric quadrupoles
   in enantiomophic ferroborate $DyFe_3(BO_3)_4$

4. Summary

Experimental setting for resonant x-ray diffraction using circularly polarized soft x-ray

- **SPring-8 BL17SU**
  - Temperature : 30K - 330K
  - Energy: 400eV - 2000eV
    (λ: 6.2Å- 31Å)
  - polarization : RCP (Helicity(+))
    LCP (Helicity(−))

by Dr. Yoshikazu Tanaka

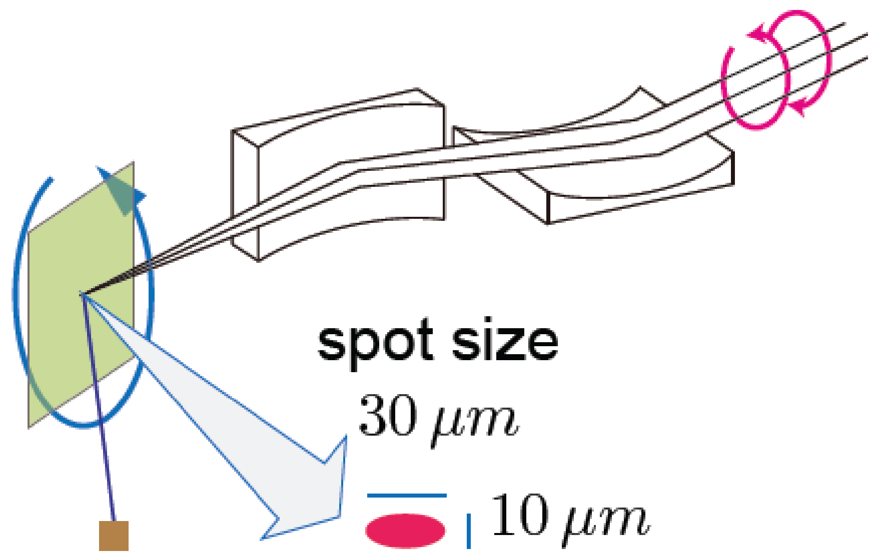

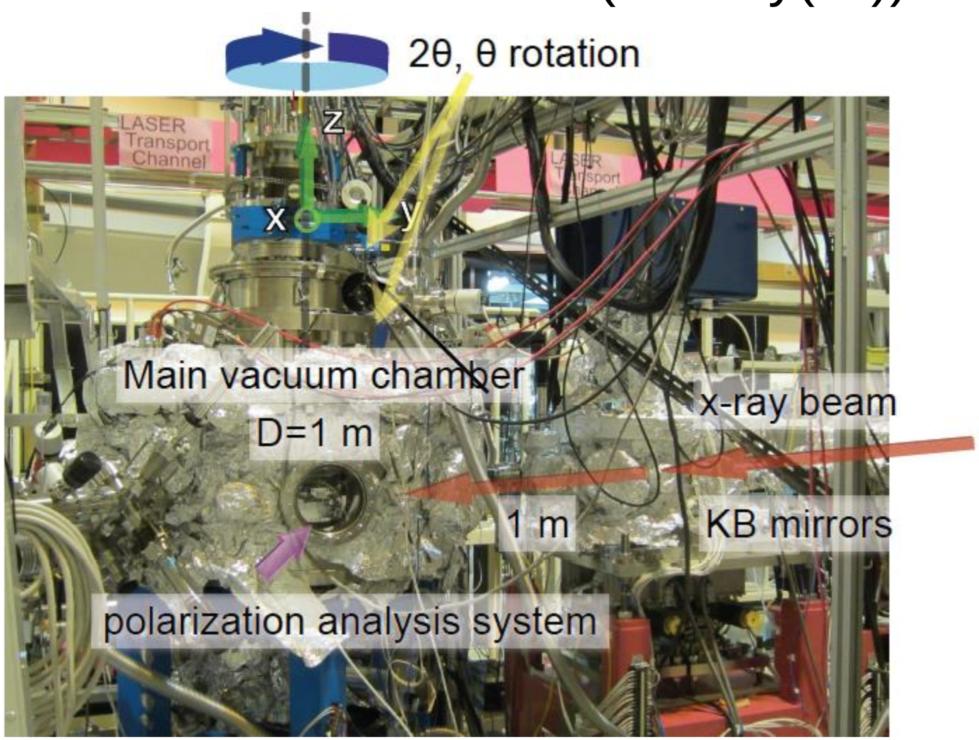

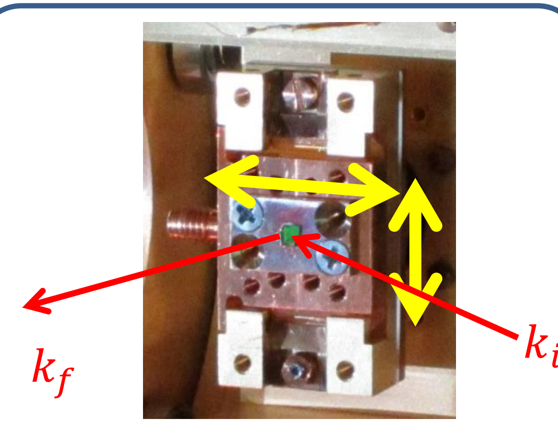

Spot size : 10μm×30μm

Magnetoelectric Y-type hexaferrite $(Ba,Sr)_2\mathit{Me}_2Fe_{12}O_{22}$ (Me=Zn, Mg, etc.)

Kimura et al., PRL. 94, 137201 (2005)

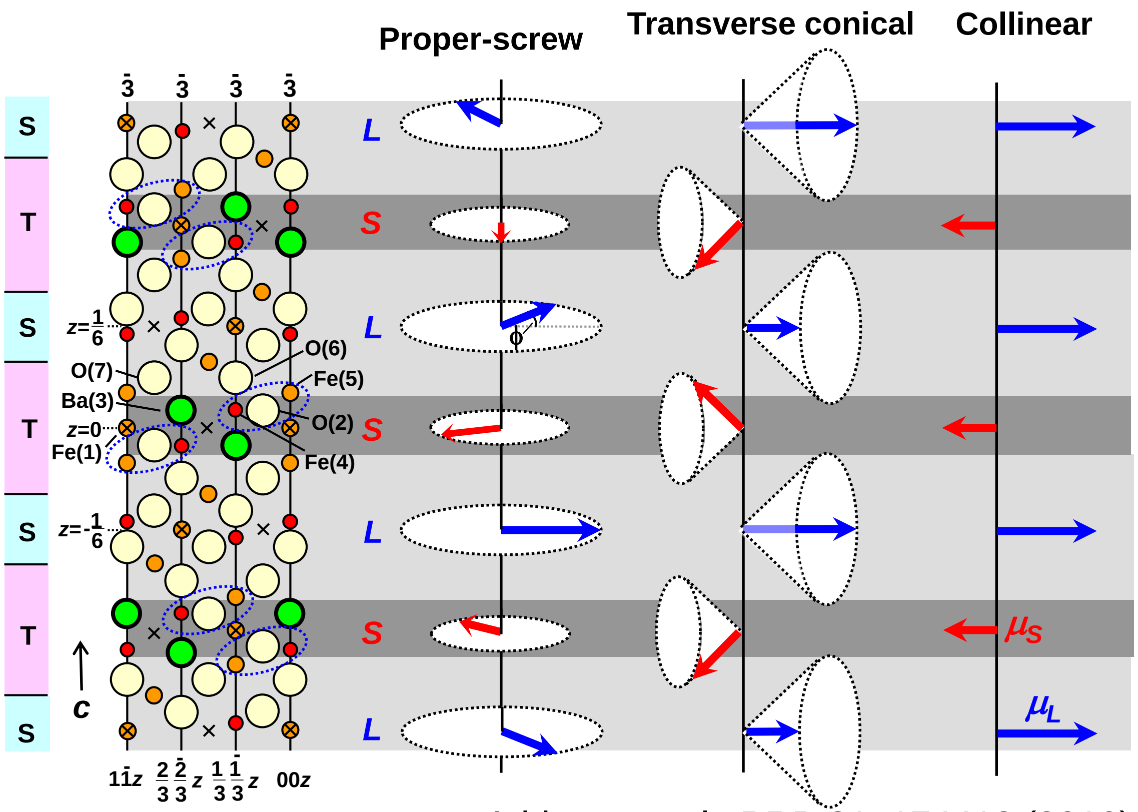

Ishiwata et al., PRB 81, 174418 (2010).

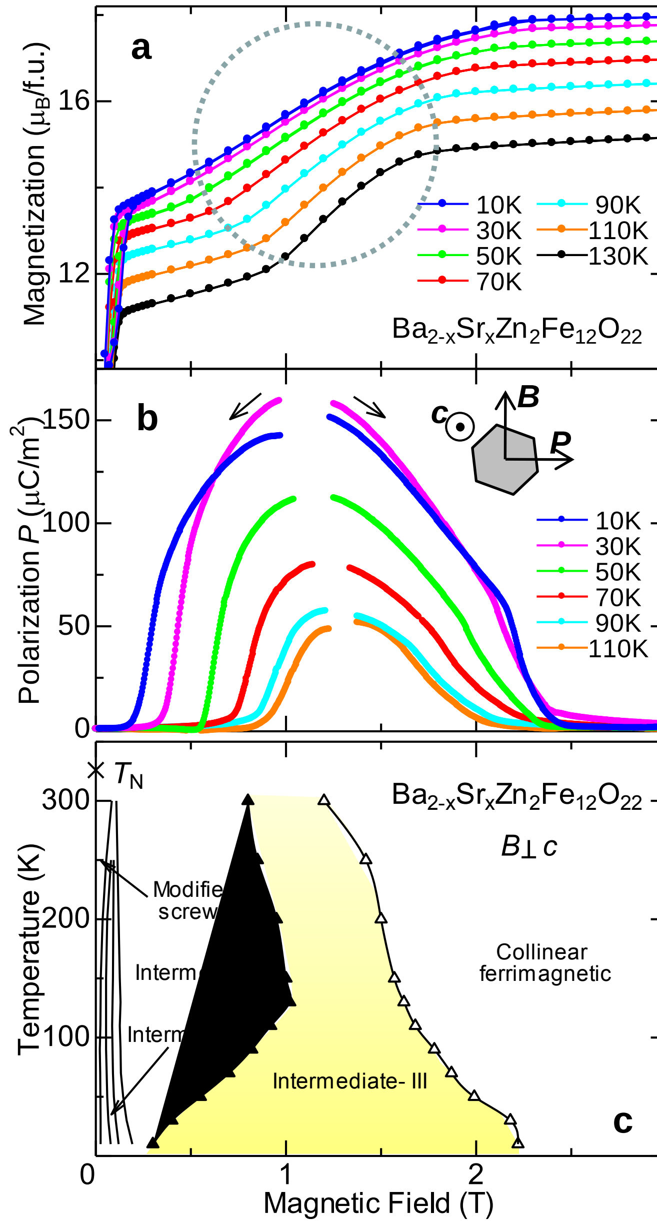

S.G. : R-3m

(extinction rule 0,0,3n)

c-axis: ~43Å

Fe L_3 edge (2p → 3d)

$h\nu$ ~ 710 eV (λ ~17 Å)

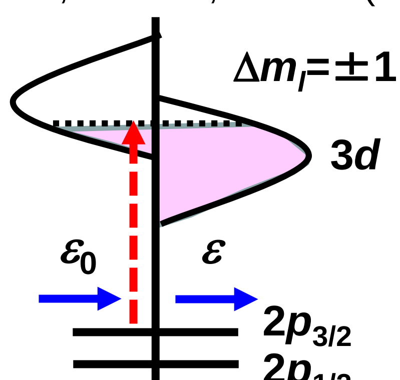

Circularly polarized x-ray diffraction study of $Ba_{0.8}Sr_{1.2}Zn_2Fe_{12}O_{22}$

Mulders et al., PRB 81, 092405 (2010).

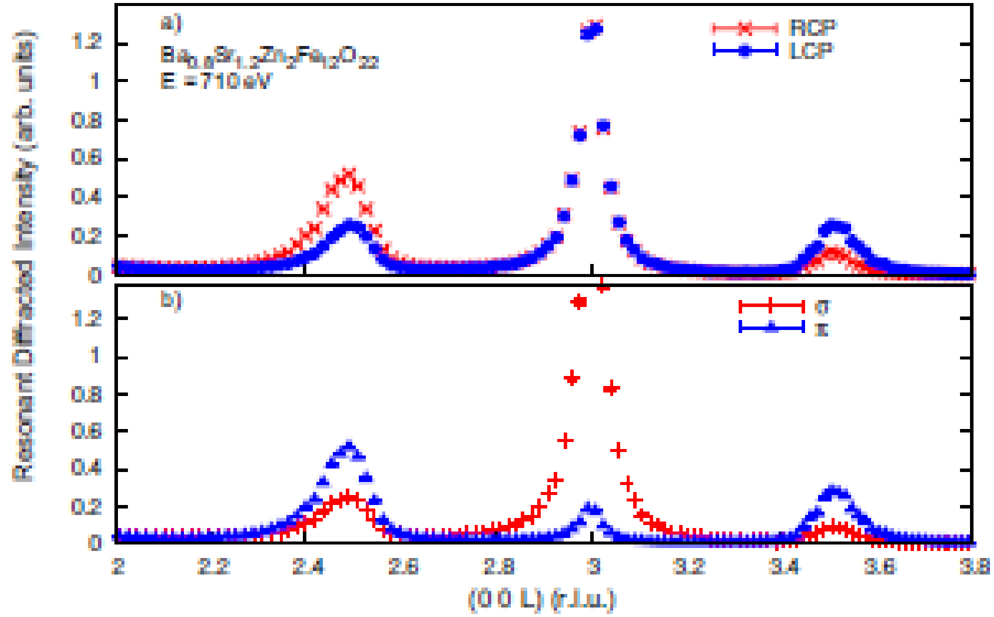

Magnetic diffraction intensity along *c* f

$$I_{right} \propto \left(\cos^2\theta + \frac{1}{2}\sin^2 2\theta \mp \chi\cos\theta\, s\right.$$

$$I_{left} \propto \left(\cos^2\theta + \frac{1}{2}\sin^2 2\theta \pm \chi\cos\theta\, s\right.$$

F_{11}, F_{1-1} : atomic prope

$\boldsymbol{q}$ (= $\boldsymbol{k}_i$ - $\boldsymbol{k}_f$), $\boldsymbol{G}$: reciproc

If the fractions of the right- and left-handed spin-chiral domains are *a* and (1-*a*), respectively

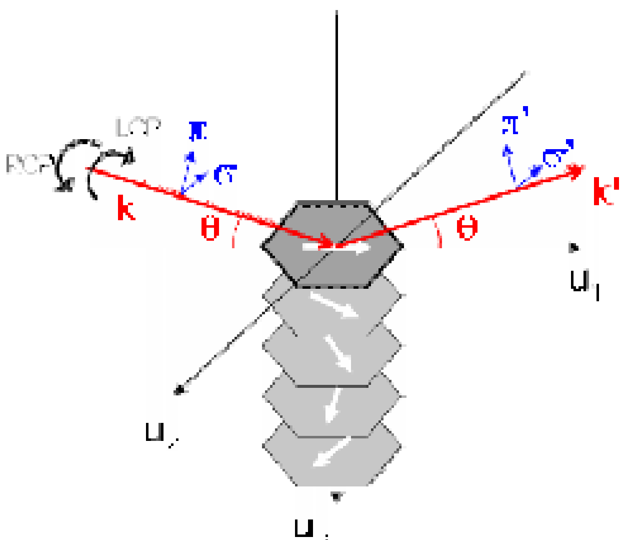

$$I_a^{(-)} \Big/ I_a^{(+)} = \frac{\cos^2\theta + \frac{1}{2}\sin^2 2\theta \mp (1-2a)\cos\theta\sin 2\theta}{\cos^2\theta + \frac{1}{2}\sin^2 2\theta \pm (1-2a)\cos\theta\sin 2\theta}.$$

	(003^-)		(003^+)	
Incident polarization	Exp.	Calc.	Exp.	Calc.
RCP	0.50	0.52	0.11	0.10
LCP	0.24	0.25	0.25	0.23

***a* = 0.77**

Imaging spin-chiral domains in Y-type $Ba_{0.5}Sr_{1.5}Zn_2Fe_{12}O_{22}$ by circularly polarized X-ray

Sample **$Ba_{0.5}Sr_{1.5}Zn_2Fe_{12}O_{22}$ T_N ~ 310 K magnetic satellite $(0,0,3n\pm\varepsilon)$**

Experimental conditions

- ***X-ray energy 710 eV [at Fe L_3 edge]**
- ***Beam size 30 x 15 μm^2**
- ***Penetration depth ~40 nm**

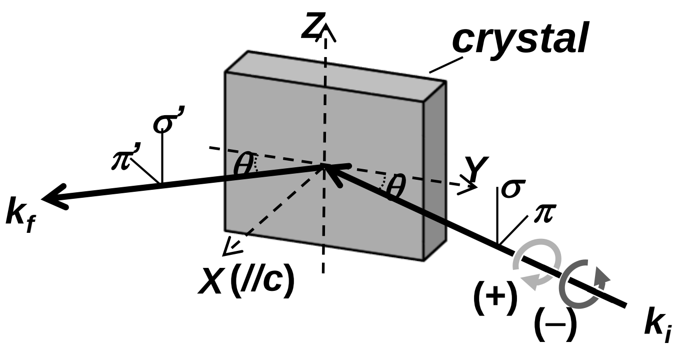

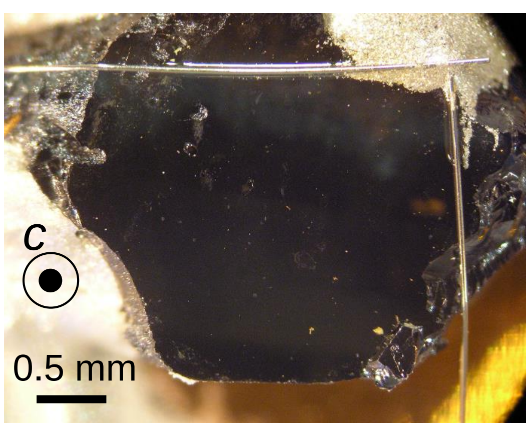

Crystal surface

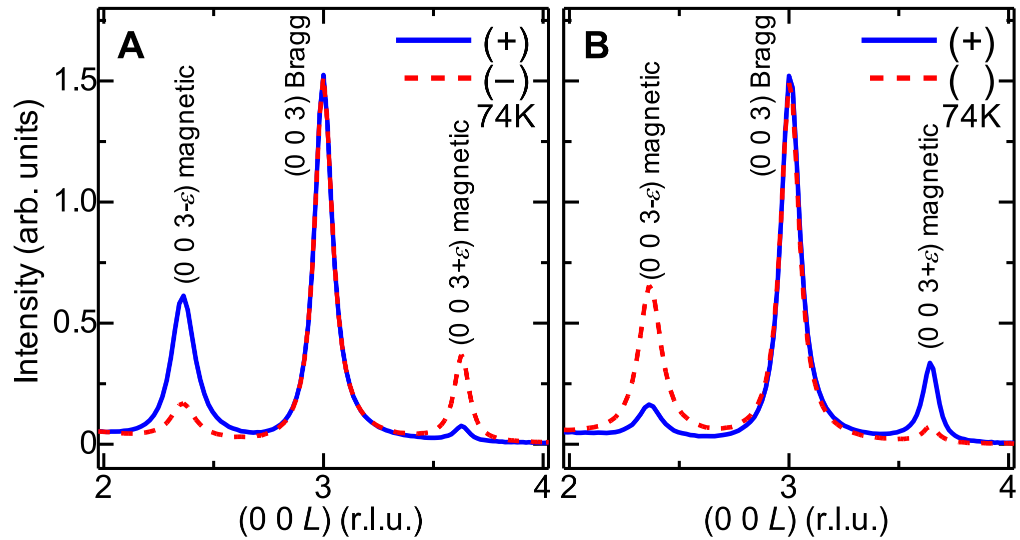

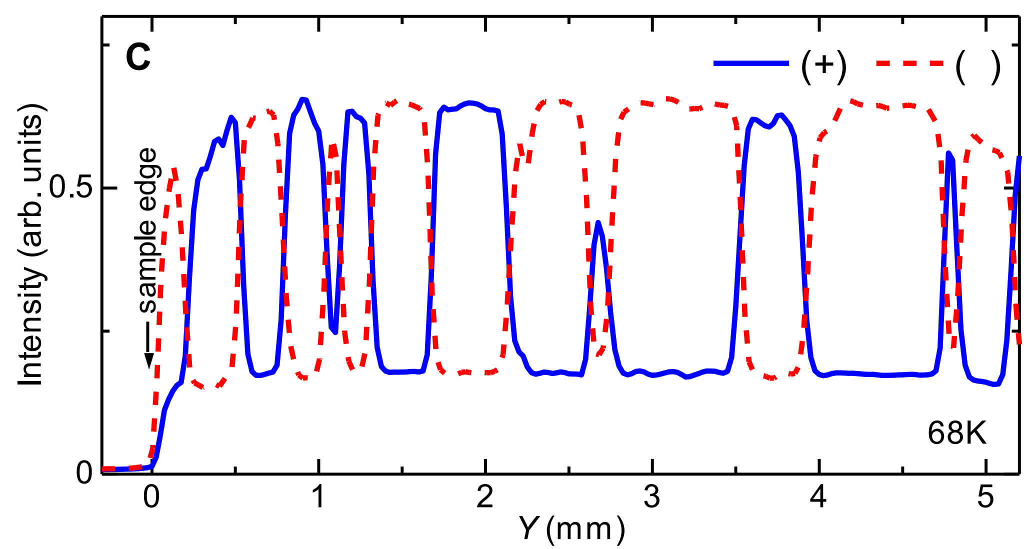

Spatial images of spin-chiral domain structure in $Ba_{0.5}Sr_{1.5}Zn_2Fe_{12}O_{22}$ at 68 K

Y. Hiraoka et al., PRB 84, 064418 (2011).

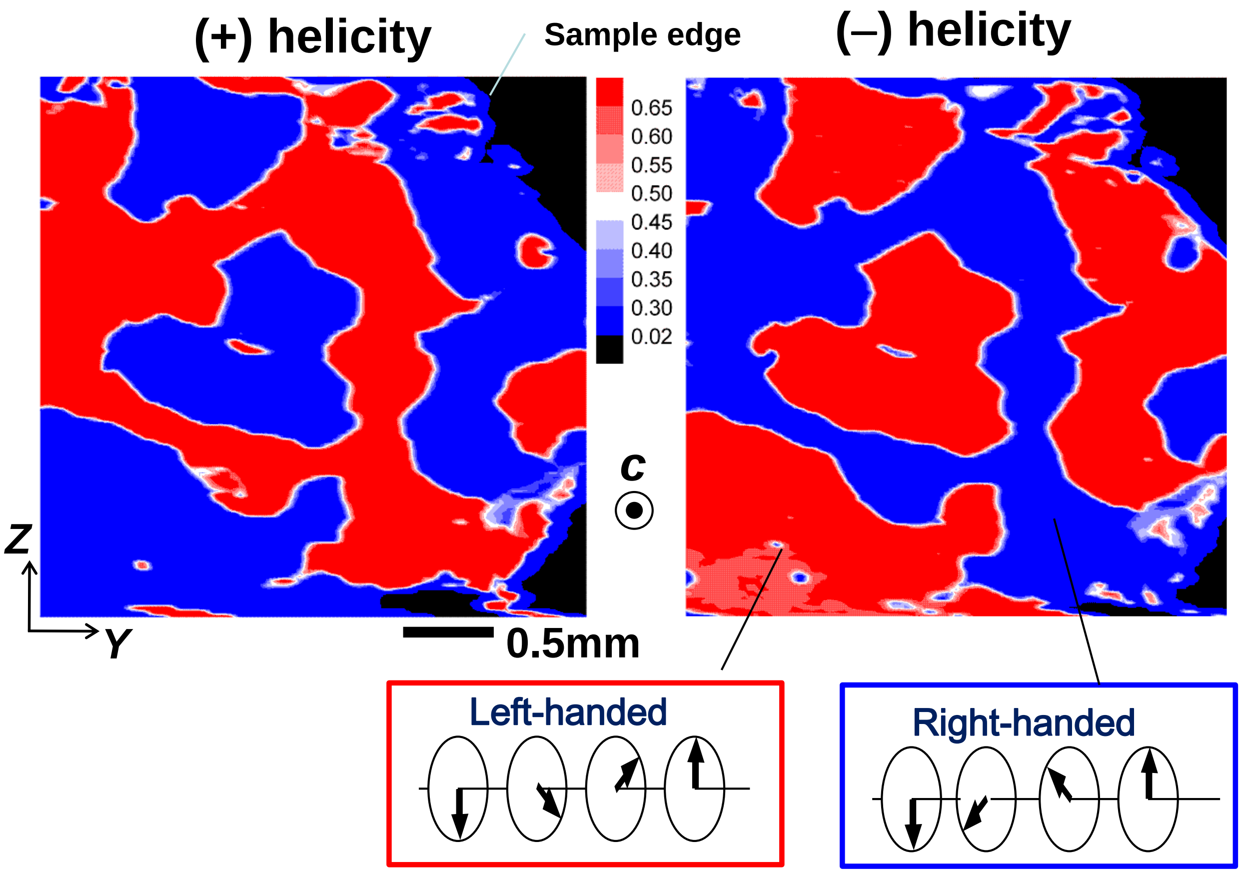

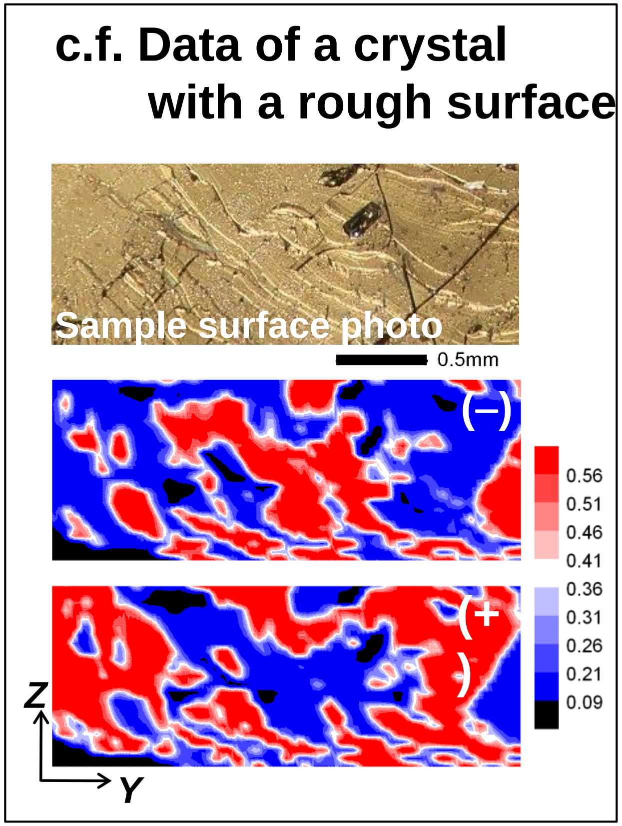

*Red and blue regions correspond to either a left- or right-handed spin-chiral monodomain.
*The observed domains are irregular in shape with a size on a submilimeter scale.

*There is a tendency that the domain boundaries are clamped at surface defects.
*The observed domains were apparently smaller in size than those on a smooth surface.

Effect of field-cooling on spin-chiral domain structure in $Ba_{0.5}Sr_{1.5}Zn_2Fe_{12}O_{22}$

Y. Hiraoka *et al.*, J. Magn. Magn. Mater. 384, 160 (2015).

We measured intensity maps of the (0 0 3−ε) magnetic reflection at 40 K after various field-cooling conditions.

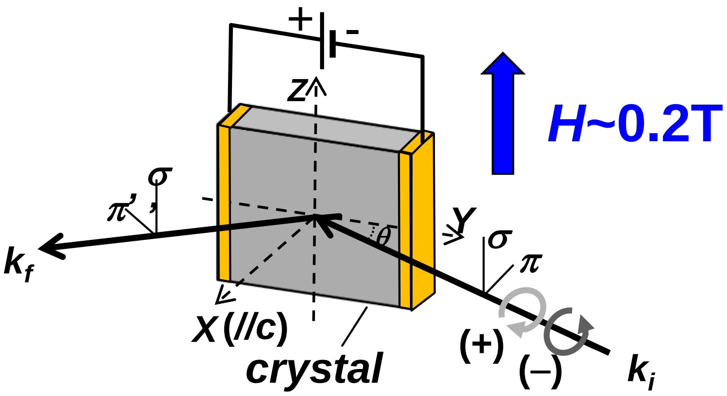

Sample is cooled from 330 K (>T_N) to 40 K at E = 0.5 ~ 200 kV/m.

With a permanent magnet, H (~0.2 T) can be applied .

During the measurement, H is removed.

After *E*-field cooling

After *H*-field cooling

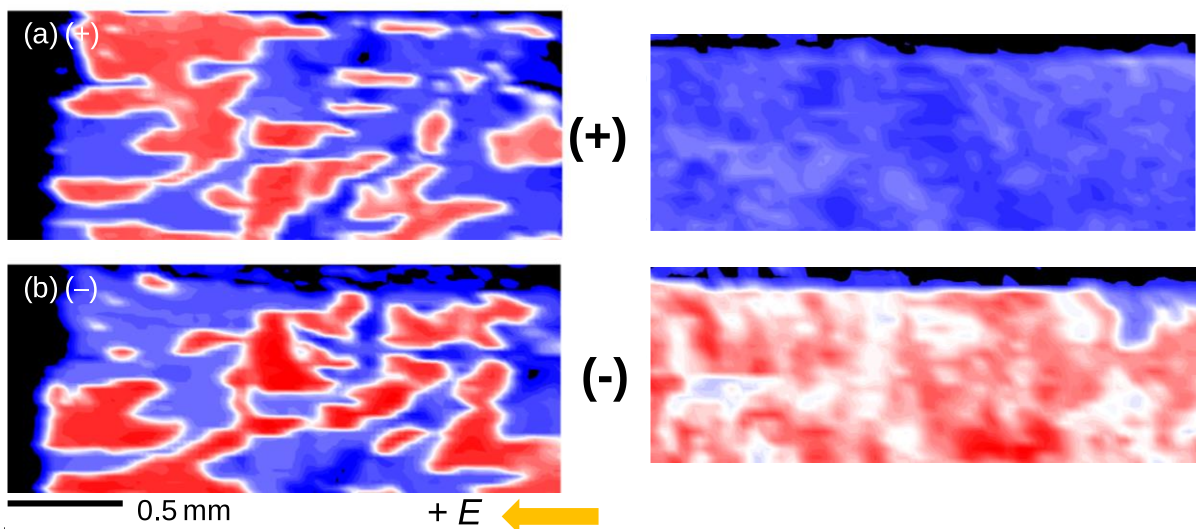

*No effect on domain structure by *E*-field cooling

By H-field cooling, the images becomes more homogeneous.

Field-cooling condition dependence of spin-chiral domain structures

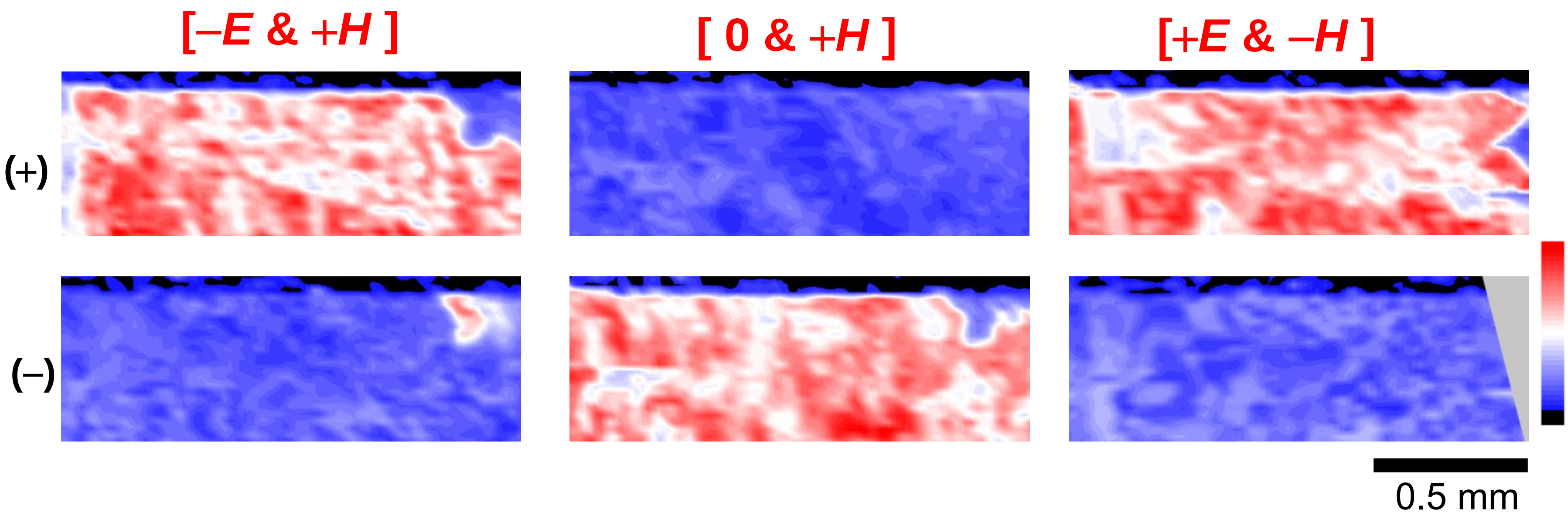

The sign of *H* is does not determine the handedness.

The penetration depth of the incident x-ray into the crystal is $\xi \approx 40$ nm. Therefore, the2D scanned intensity maps only reflect the spin-chiral state only at nearby surface.

Possible formation of spin-chiral domains with “stripe-type” domain walls

Polarized neutron topographs of a Tb single crystal

Tb metal

Baruchel et al., J. Physique 49-C8, 1895 (1988).

(spiral axis // hexagonal *c* axis)

F-domain →   ← P-domain

Ferromagnetic | *Helimagnetic* | *Paramagnetic*

221K   229K   ***T***

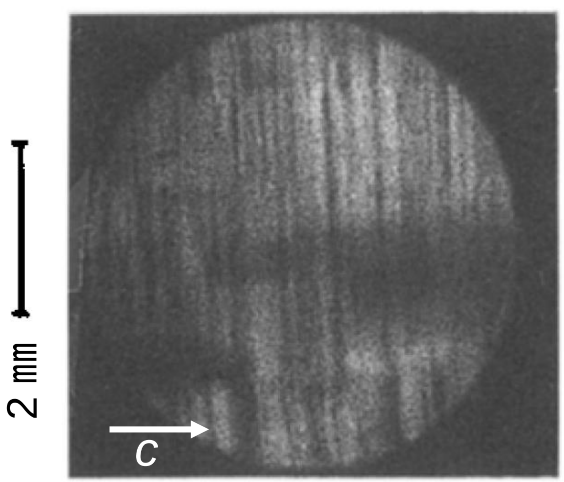

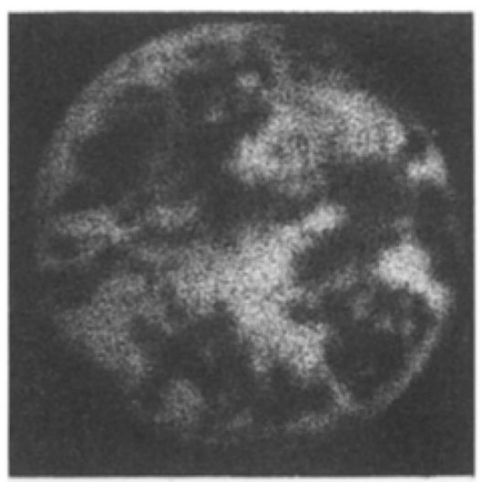

Stripe-shaped F-domain

Curved wall P-domain

Phase diagram of $Ba_{0.5}Sr_{1.5}Zn_2Fe_{12}O_{22}$

Kimura et al. PRL (2005)

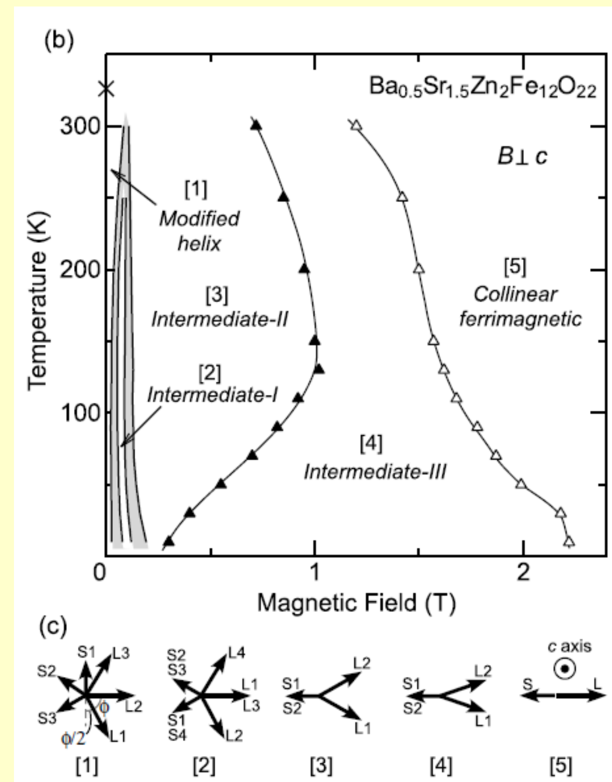

By *H*-field cooling procedure, the spiral phase appears after a ferromagnetic one.

Outline of this presentation

Observation of multipole helix-chiral domains by resonant x-ray scattering

1. Resonant x-ray diffraction using circularly polarized x-rays
   a technique to verify symmetry breaking due to chirality

2. Chiral domains due to magnetic dipoles in multiferroic
   Y-type hexaferrites $(Ba,Sr)_2Z(Co,Zn)_2(Fe,Al)_{12}O_{22}$

3. Chiral domains due to electric quadrupoles
   in enantiomophic ferroborate $DyFe_3(BO_3)_4$

4. Summary

$RFe_3(BO_3)_4$ (R = Rare earth)

- Single crystals
  - R = Y, La, Pr, Nd, Sm,
    Eu, Gd, Tb, Dy, Ho, Er

- Structural phase transition
  space group $R32 \rightarrow P3_121$ or $P3_221$
  - R = Eu, Gd, Tb, Dy, Ho, Er, Y

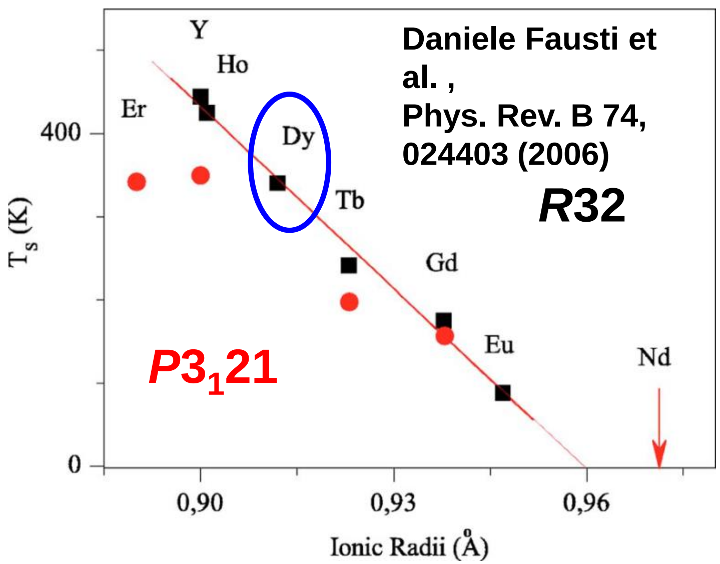

■ : Poly sample
● : Single crystal by $Bi_2Mo_3O_{12}$-based flux

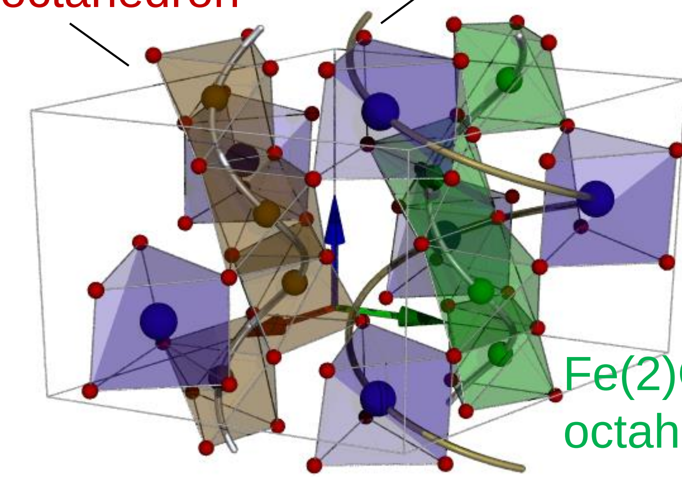

$P3_221$ (~T_S=285K)
a = 9.5439 [Å] c = 7.5676 [Å]

C Ritter, et al. , Phys. : Conf. Ser. 340, 012065 (2012)

R32

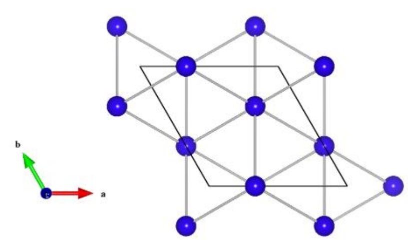

$P3_121$

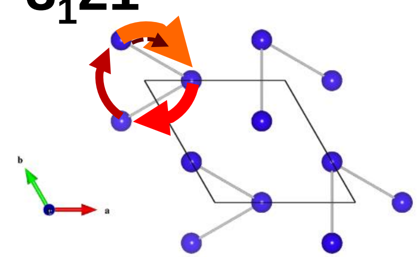

$DyFe_3(BO_3)_4$

Growth and characterization of $DyFe_3(BO_3)_4$

Single crystals were grown in Bi_2O_3 based flux.

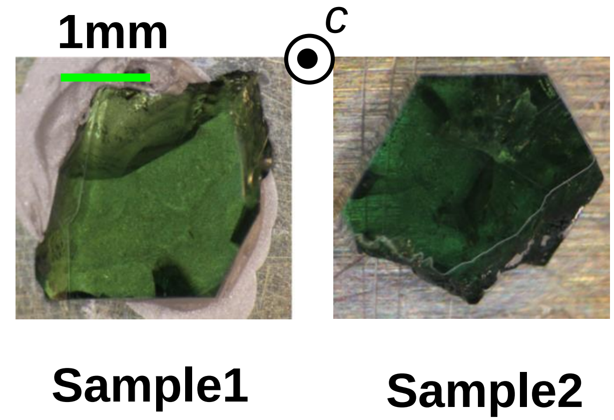

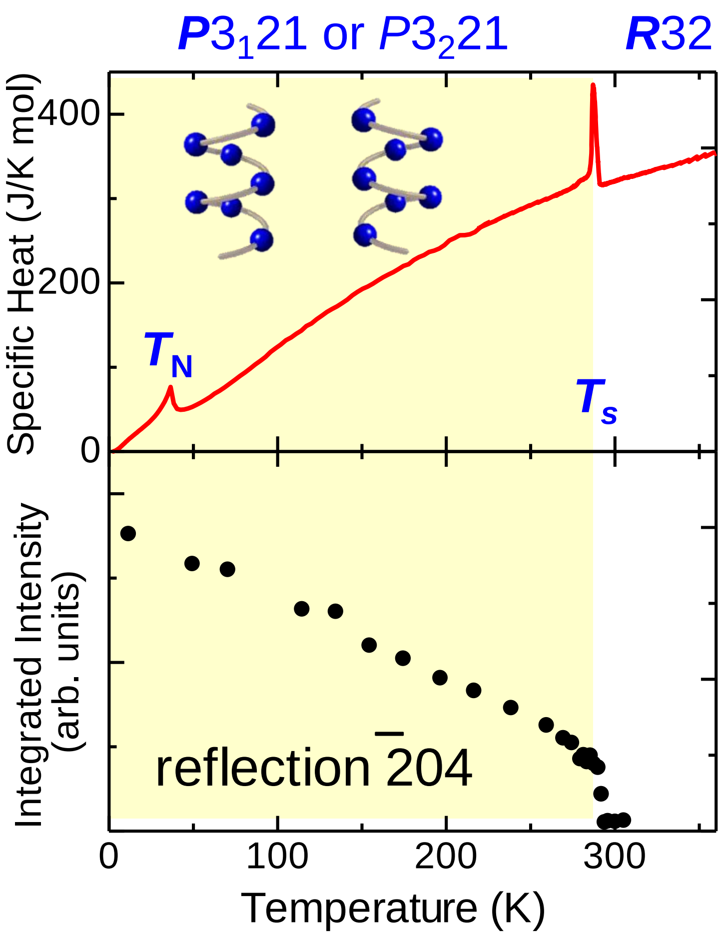

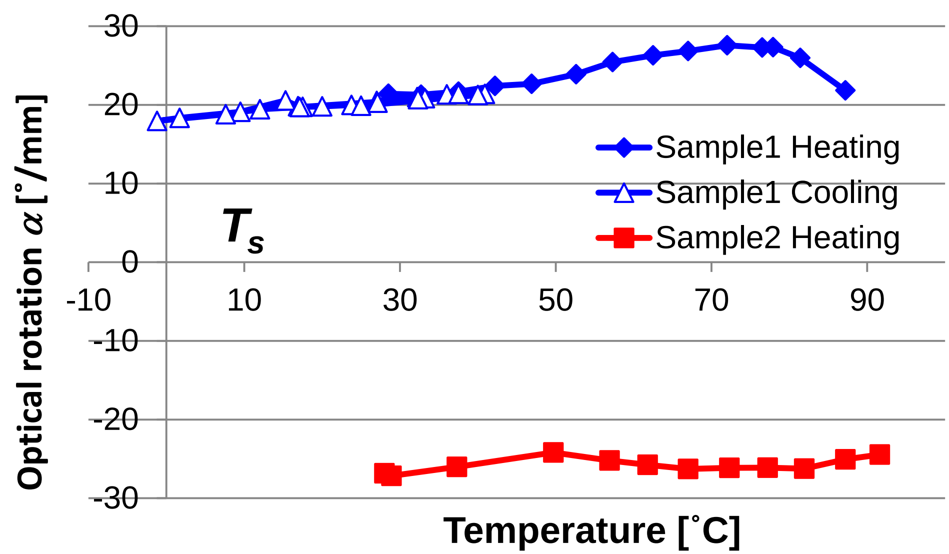

Magnetism and magnetoelectricity in $DyFe_3(BO_3)_4$

Powder neutron diffraction

Ritter et al., J. Phys. Conf. 340, 012065 (2012).

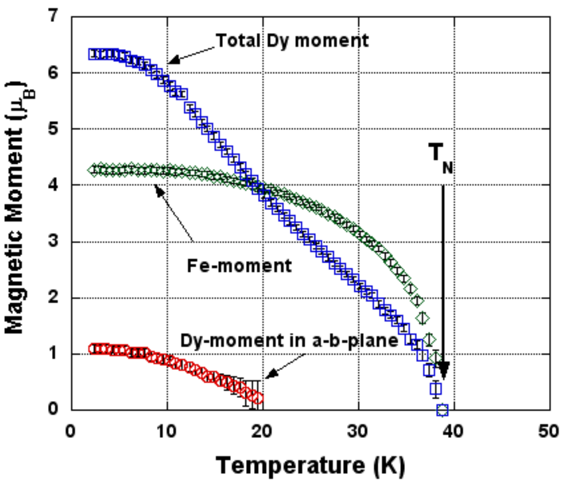

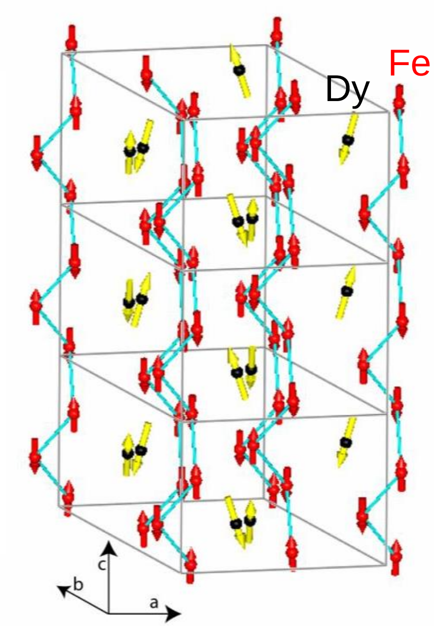

Antiferromagnetic below T_N = 38K

for both Fe and Dy moments

predominantly easy-axis type

with wave vector [00½]

Below 20 K

a small component forming

a 120° type arrangement of Dy moments

ME effect related to spin flop

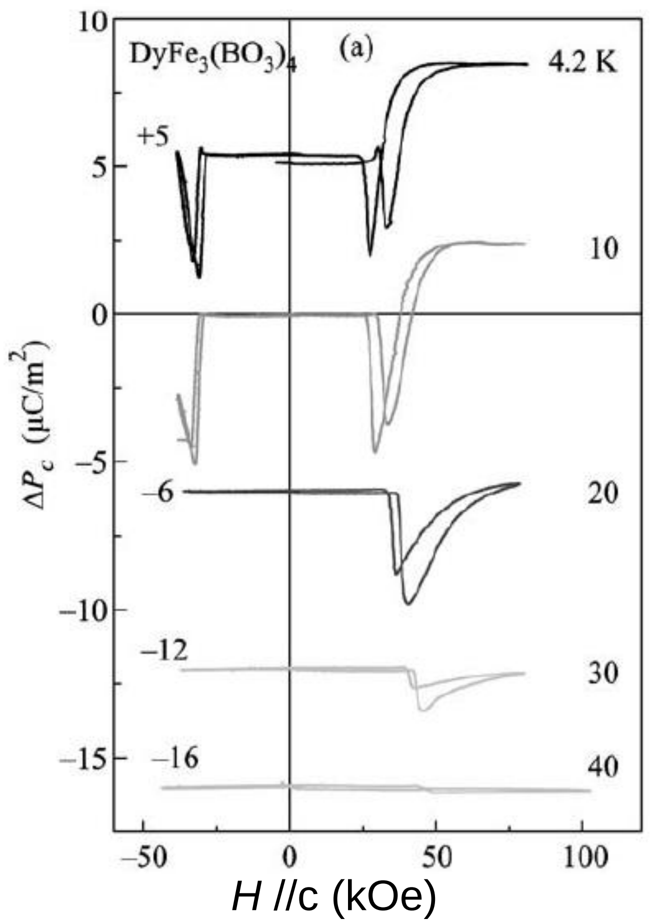

Popov et al., JETP Lett. 89, 345 (2009)

Spectra of the x-ray absorption and forbidden reflection 001

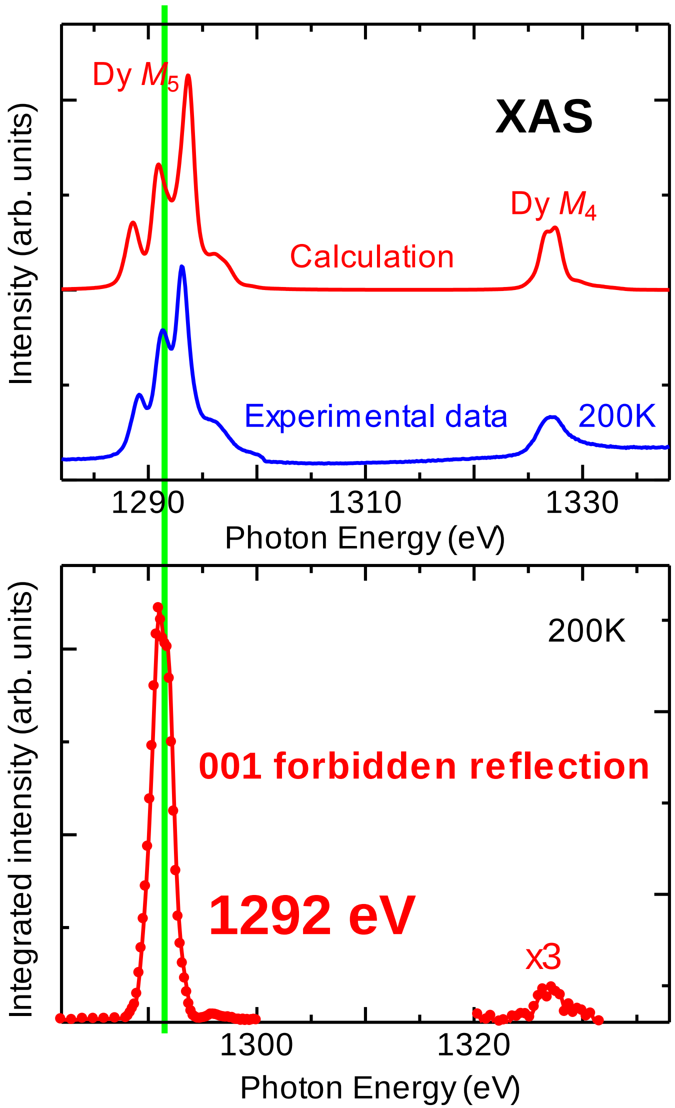

Calculated XAS spectra to the Dy 3*d*-4*f* electric dipole (E1) transitions

The calculations are atomic multiplet calculations for the Dy^{3+} free ion for paramagnetic spin state.

001 reflection studied here is dominated by the *E*1*E*1 transition

X-ray helicity dependence

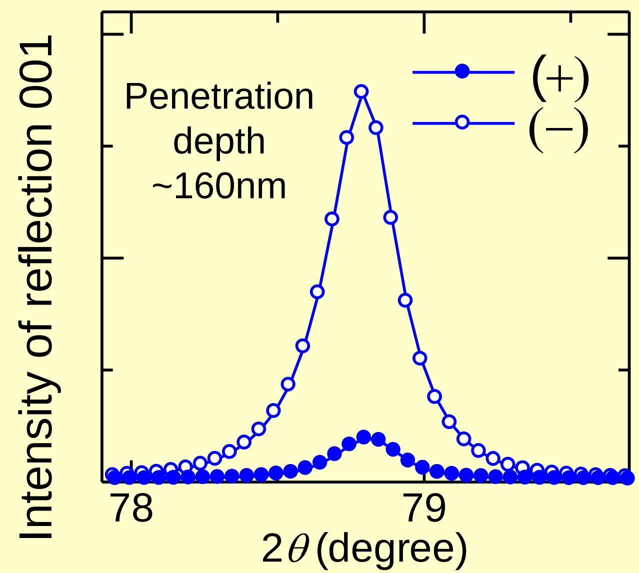

2D *yz*-scanned intensity map of forbidden reflection 001

Sample #1

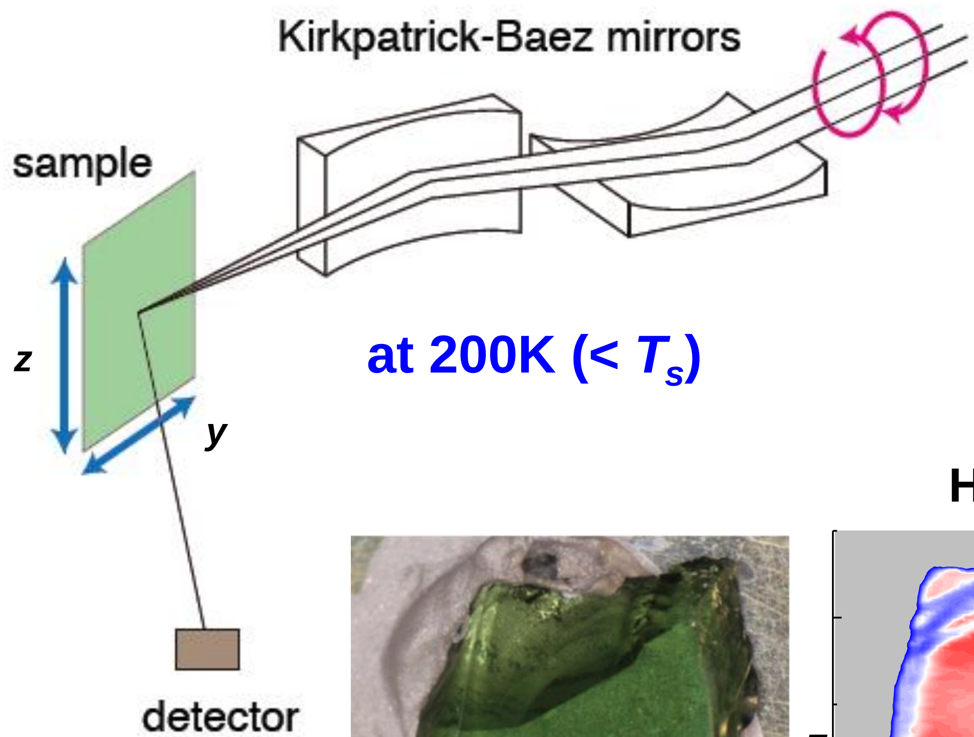

at 200K (< T_s)

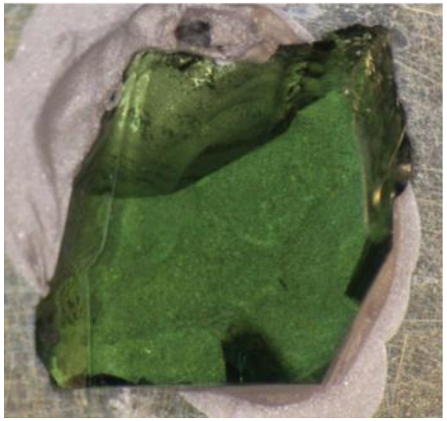

Sample #1

Helicity (–)

Helicity (+)

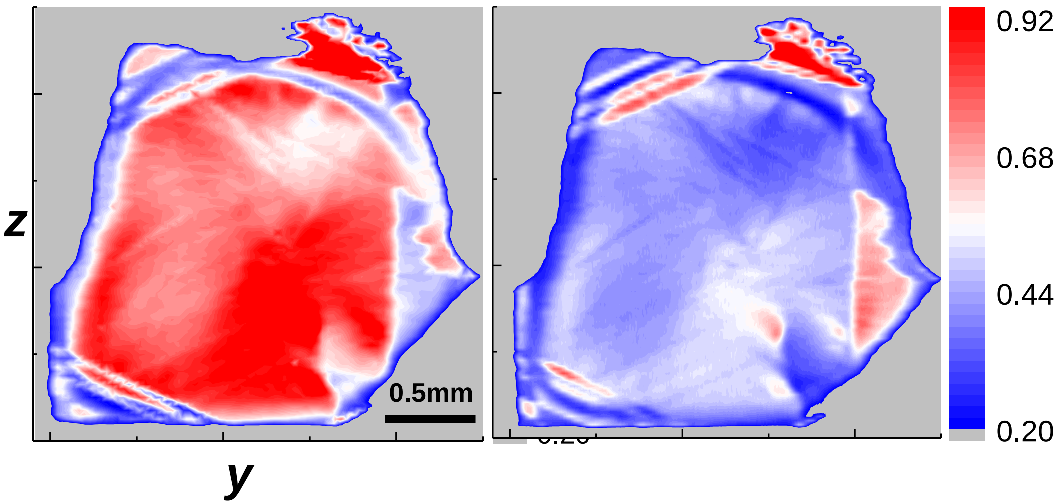

Nearly a single domain with left screw structure ($P3_221$)

2D *yz*-scanned intensity map of forbidden reflection 001
Sample #2

Usui et al., Nature Mater. 13, 611 (2014)

at 200K (<T_s)

(–) helicity **(+) helicity**

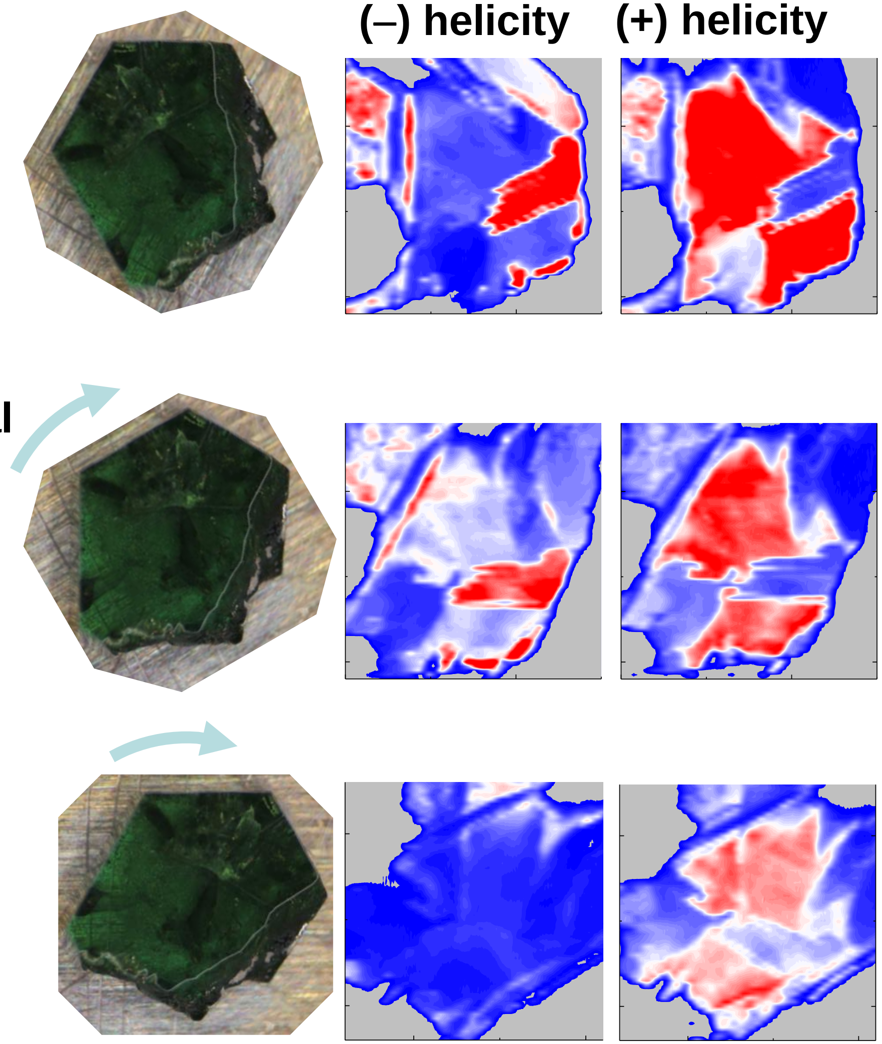

Rotation of azimuthal angle

Multi-domain structure

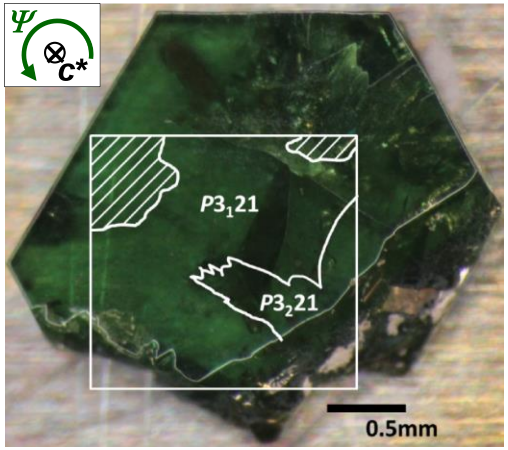

Theoretical descriptions of the structural factor for the enantiomorphic space group pair

S. W. Lovesey et al. ,J. Phys.: Condens. Matter 20 (2008) 272201

Azimuthal angle dependence of the (001) reflection intensity in the enantiomorphic space group pair $P3_121$ and $P3_221$ for the E_1E_1 resonant event

$$I = I_0 + I_1\cos(3\Psi) \boxed{+ I_2\sin(3\Psi)}$$

$\leftarrow$ originating from an odd parity event such as E1E2 event

$$I_0 = \frac{1}{2}\{T_a^2(1+\sin^2\theta)^2 + T_\beta^2\} + \frac{1}{2}P_3T_a^2(1+\sin\theta)^2\cos^2\theta + P_2\nu T_a^2\sin\theta\,(1+\sin^2\theta) \quad (2)$$

$$I_1 = 2P_3\nu T_a T_\beta \sin\theta - P_2 T_a T_\beta \cos^2\theta. \quad (3)$$

where $T_a = \frac{3}{2}\langle T_{+2}^2\rangle'$ and $T_\beta = \frac{3}{2}\langle T_{+1}^2\rangle''\cos\theta$. *$\leftarrow$2-types of quadrupole moments*

P_2 and P_3 : Stokes parameter

$P_2 = +0.944\ (-0.944)$ and $P_3 = -0.164$ for + (-) helicity x-rays.

ν : Chirality $\nu = +1$ ($P3_121$) or $\nu = -1$ ($P3_221$)

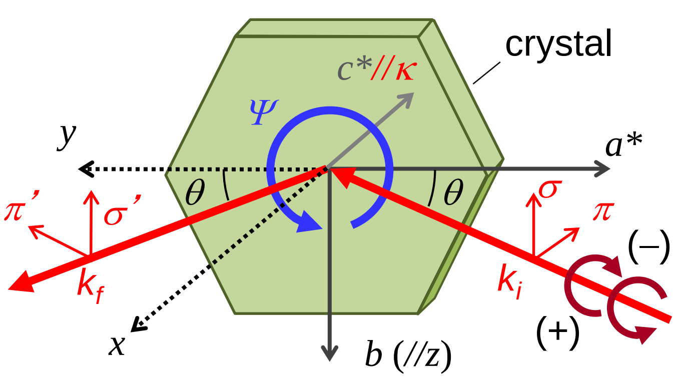

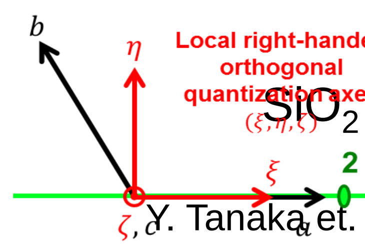

Y. Tanaka et. al , PRL 100 , 145502 (2008)

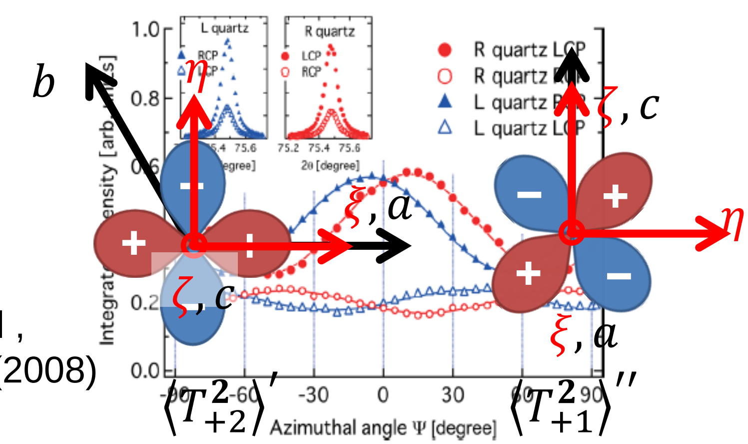

Azimuthal angle dependence in $DyFe_3(BO_3)_4$

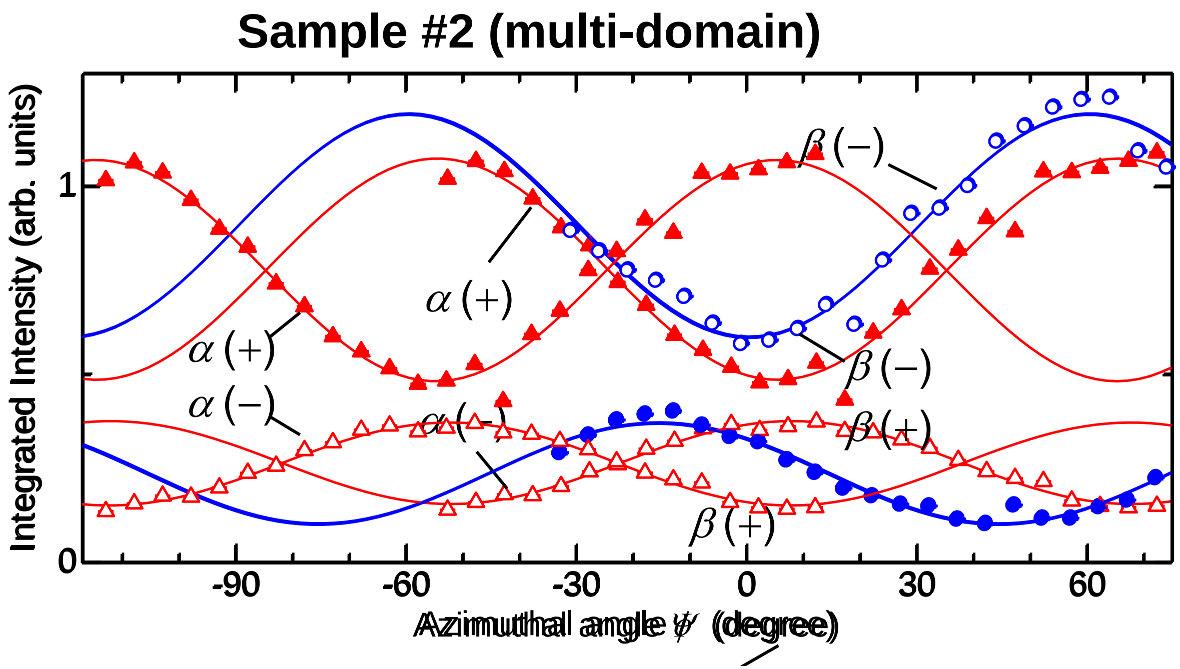

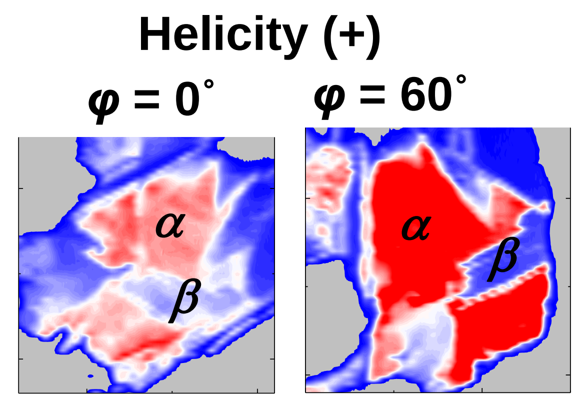

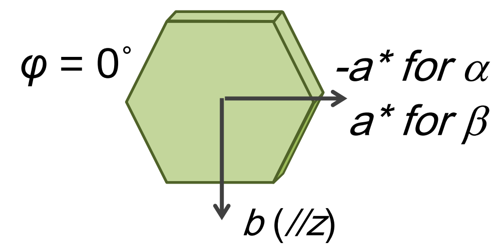

Region	ν (S.G.)	P_2	I_0^{exp}	I_0^{cal}	I_1^{exp}	I_1^{cal}
α	+1 ($P3_121$)	−0.944	0.264	$0.012T_\alpha^2 + T_\beta^2$	−0.110	$0.353T_\alpha T_\beta$
		+0.944	0.778	$1.70T_\alpha^2 + T_\beta^2$	0.294	$-0.770T_\alpha T_\beta$
β	−1 ($P3_221$)	−0.944	0.895	$1.70T_\alpha^2 + T_\beta^2$	−0.297	$-0.770T_\alpha T_\beta$
		+0.944	0.236	$0.012T_\alpha^2 + T_\beta^2$	0.134	$0.353T_\alpha T_\beta$

Temperature evolution of azimuthal angle dependence

Sample #1 Left-screw mono-domain

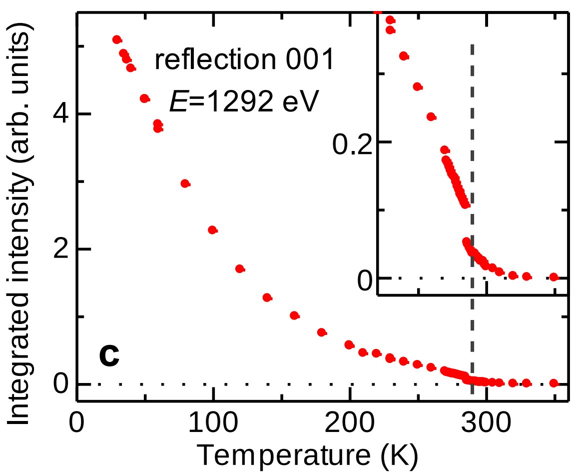

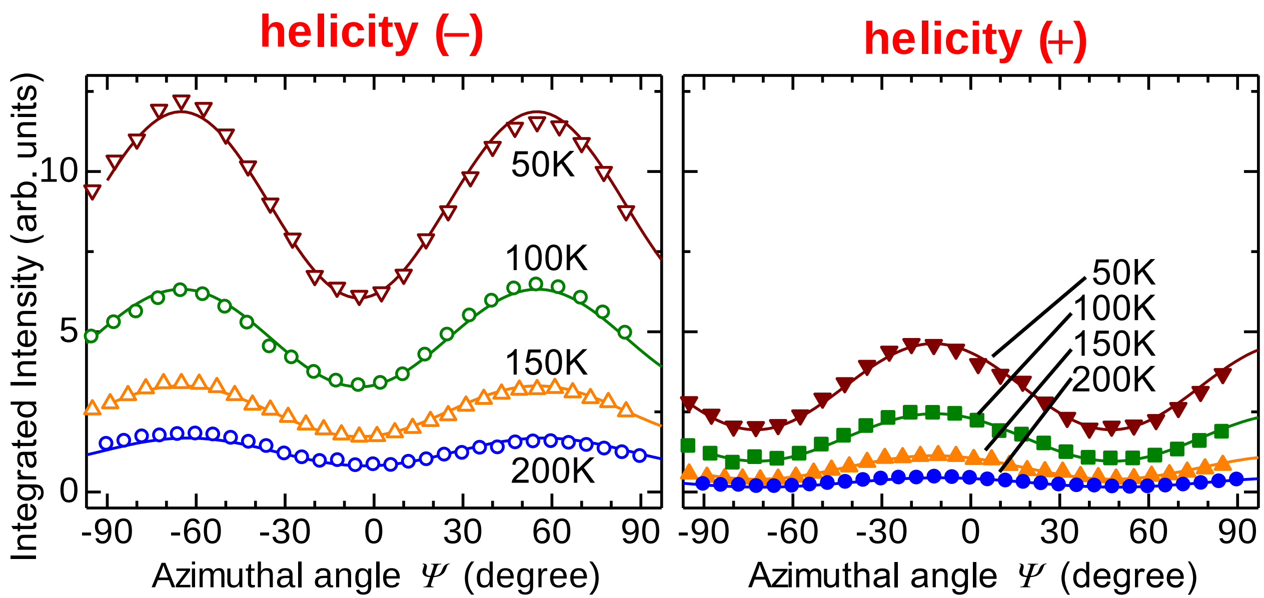

T (K)	P_2	I_0^{exp}	I_0^{cal}	I_1^{exp}	I_1^{cal}	T_a^2	T_β^2	$-T_aT_\beta$	$\frac{\langle T_{+2}^2\rangle'}{\langle T_{+1}^2\rangle''}$
200	-0.944	1.25	$1.70T_a^2+T_\beta^2$	0.434	$-0.770T_aT_\beta$	~0.6	~0.3	0.4~0.5	~1.1
	$+0.944$	0.297	$0.012T_a^2+T_\beta^2$	-0.146	$0.353T_aT_\beta$				
150	-0.944	2.52	$1.70T_a^2+T_\beta^2$	0.795	$-0.771T_aT_\beta$	~1.0	~0.8	0.9~1.0	~0.91
	$+0.944$	0.765	$0.012T_a^2+T_\beta^2$	-0.366	$0.354T_aT_\beta$				
100	-0.944	4.80	$1.70T_a^2+T_\beta^2$	1.52	$-0.771T_aT_\beta$	~1.8	~1.7	1.8~2.0	~0.81
	$+0.944$	1.70	$0.012T_a^2+T_\beta^2$	-0.741	$0.354T_aT_\beta$				
50	-0.944	8.94	$1.70T_a^2+T_\beta^2$	2.92	$-0.771T_aT_\beta$	~3.4	~3.2	3.3~3.7	~0.79
	$+0.944$	3.29	$0.012T_a^2+T_\beta^2$	-1.31	$0.354T_aT_\beta$				

Electronic structure of Dy^{3+} 4*f* electrons in $DyFe_3(BO_3)_4$

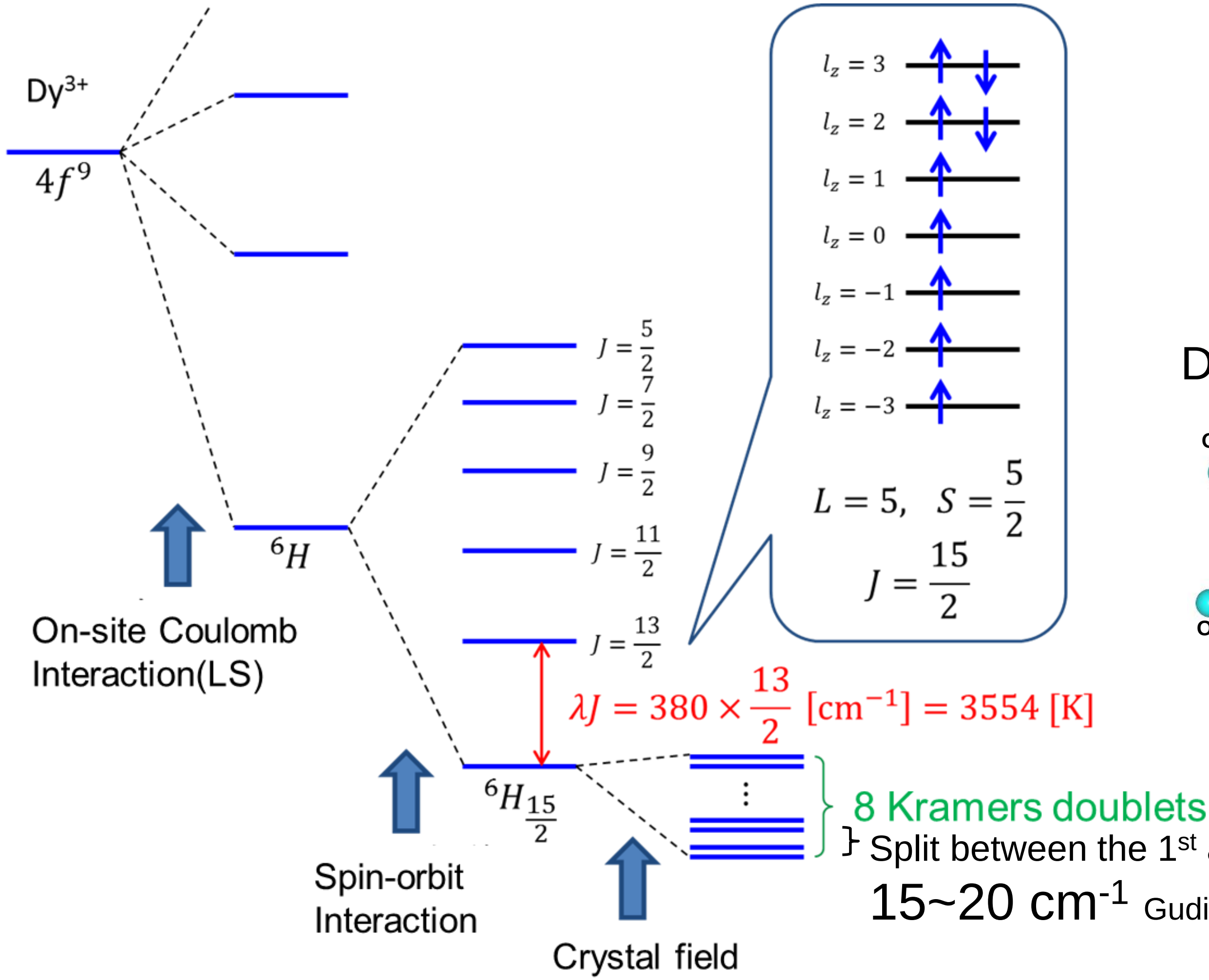

} Split between the 1st and 2nd sublevels

15~20 cm^{-1} Gudim et al. Phys. Lett. A 368, 408 (2007)

DyO_6 prism

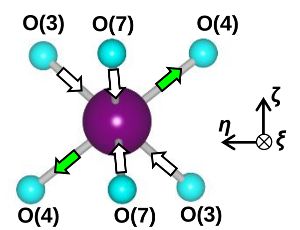

The temperature evolution of the intensity of reflection 001 may be affected by the population at the respective sublevels.

Proposed quadrupole helix chirality in $DyFe_3(BO_3)_4$

Results of
crystal structure analysis

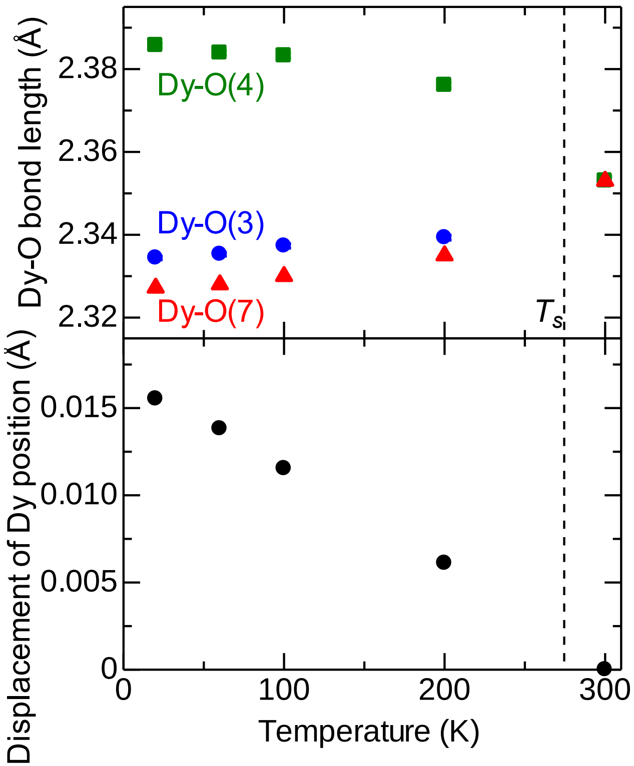

by N. Katayama, H. Sawa

BL02B1, SPring-8

$P3_221$
(Left-handed screw)

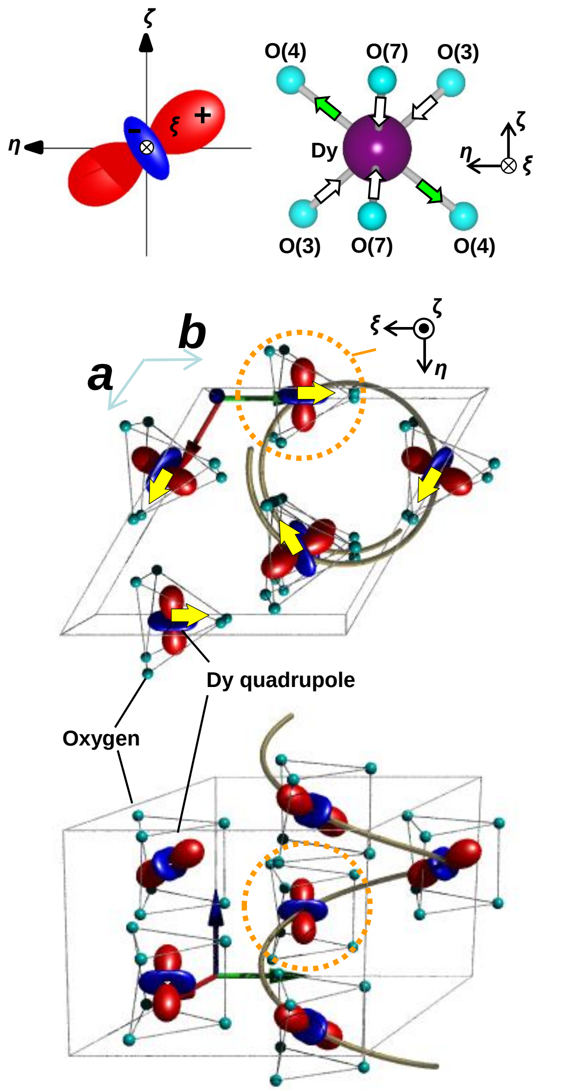

$P3_121$
(Right-handed screw)

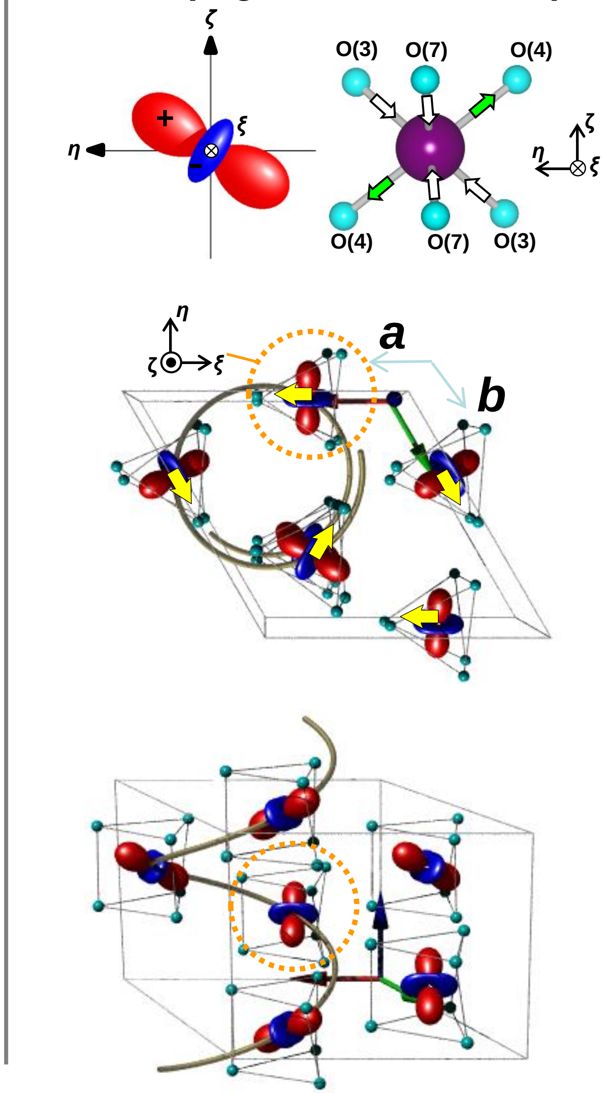

Summary

Observation of multipole helix-chiral domains by resonant x-ray scattering

*Chiral domains due to magnetic dipoles in multiferroic hexaferrite $Ba_{0.5}Sr_{1.5}Zn_2Fe_{12}O_{22}$

Hiraoka et al., PRB 84, 064418 (2011); Hiraoka et al, JMMM 384, 160 (2015).

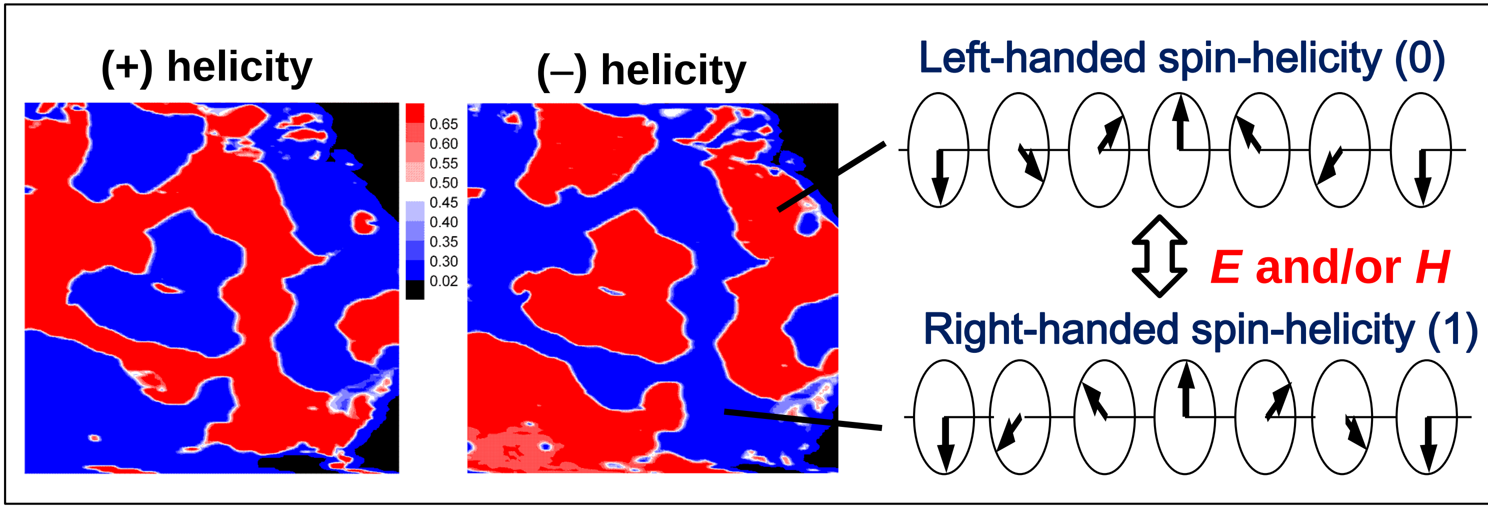

*Chiral domains due to electric quadrupoles in enantiomophic ferroborate $DyFe_3(BO_3)_4$

Usui et al., Nature Mater. 13, 611 (2014)